USED FUEL DISPOSITION CAMPAIGN

Test Plan for Investigation of Material Interactions in Heated Salt

Fuel Cycle Research & Development

Prepared for
U.S. Department of Energy
Used Fuel Disposition Campaign

Christine Stockman (SNL)
David Enos (SNL)
Philippe Weck (SNL)

November 20, 2012

FCRD-USED-2013-000030

Disclaimer

This information was prepared as an account of work sponsored by an agency of the U.S. Government. Neither the U.S. Government nor any agency thereof, nor any of their employees, makes any warranty, expressed or implied, or assumes any legal liability or responsibility for the accuracy, completeness, or usefulness, of any information, apparatus, product, or process disclosed or represents that its use would not infringe privately owned rights. References herein to any specific commercial product, process, or service by trade name, trade mark, manufacturer, or otherwise, does not necessarily constitute or imply its endorsement, recommendation, or favoring by the U.S. Government or any agency thereof. The views and opinions of the authors expressed herein do not necessarily state or reflect those of the U.S. Government or any agency thereof.

FCT Quality Assurance Program Document

Name/Title of Deliverable/Milestone	Test Plan for Investigation of Material Interactions in Heated Salt/ M3FT-13SN08180342
Work Package Title and Number	DR Salt R&D - SNL, FT-13SN081803
Work Package WBS Number	1.02.08.18
Responsible Work Package Manager	Christi Leigh
	(Name/Signature)

Date Submitted 11/20/2012

Quality Rigor Level for Deliverable/Milestone	☐ QRL-3	☐ QRL-2	☐ QRL-1 ☐ Nuclear Data	☒ N/A*

This deliverable was prepared in accordance with   Sandia National Laboratories
                                                                              (Participant/National Laboratory Name)

QA program which meets the requirements of
        ☒ DOE Order 414.1   ☐ NQA-1-2000
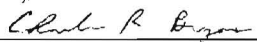
This Deliverable was subjected to:
☒ Technical Review   ☐ Peer Review

Technical Review (TR)   **Peer Review (PR)**

Review Documentation Provided   **Review Documentation Provided**
☐ Signed TR Report or,   ☐ Signed PR Report or,
☐ Signed TR Concurrence Sheet or,   ☐ Signed PR Concurrence Sheet or,
☒ Signature of TR Reviewer(s) below   ☐ Signature of PR Reviewer(s) below

Name and Signature of Reviewers
Charles Bryan

---

*Note: *In some cases there may be a milestone where an item is being fabricated, maintenance is being performed on a facility, or a document is being issued through a formal document control process where it specifically calls out a formal review of the document. In these cases, documentation (e.g., inspection report, maintenance request, work planning package documentation or the documented review of the issued document through the document control process) of the completion of the activity along with the Document Cover Sheet is sufficient to demonstrate achieving the milestone. QRL for such milestones may be also be marked N/A in the work package provided the work package clearly specifies the requirement to use the Document Cover Sheet and provide supporting documentation.*

SUMMARY

This test plan fulfills the level three mile-stone M3FT-13SN08180342, "Test Plan for Investigation of Material Interactions in Heated Salt" under Work Package Number FT-13SN081803.

In March of 2012, the United States (U.S.) Department of Energy (DOE) issued a "Salt Research and Development Study Plan" whose goal was to constructively advance generic salt repository science. Included in that plan were modeling and laboratory studies that would be necessary to build a safety case for disposal of DOE-owned and civilian high-level waste and used nuclear fuel in a generic salt repository. Task 3.5 of the study plan is to provide a test plan to investigate the interaction of brine, salt and emplacement materials in a heat-generating disposal system, with a focus on the common metals used in waste disposal operations. Corrosion of metals due to brine/salt interactions and the resulting corrosion products play primary roles in defining the near-field chemical environment, specifically the reduction/oxidation conditions, the pH, and the gas (i.e. H_2) generation rate. These parameters play key roles in determining the solubility of radionuclides and the movement of gas and brine within the repository.

In this report, a literature survey is summarized that identifies relevant information on brine/salt-materials interactions in the temperature range expected in a heat-generating disposal system. This review focuses on the major metals of the waste package, carbon steel and stainless steel, as there are few other metals in the designs of generic salt repositories (Sevougian et al., 2012). Carbon steel has been extensively investigated as a corrosion allowance waste package material for high temperature salt repositories and this literature is summarized. Stainless steel undergoes localized corrosion and stress corrosion cracking in salt environments, so has been rejected as a material for waste confinement in salt repositories. For this reason, there is little relevant literature on stainless steels. However stainless steel will most likely be used for handling of the spent nuclear fuel, and will be present in the repository in significant amounts. Corrosion of stainless steel will produce H_2 gas for longer periods than carbon steel, which may impact repository performance. Therefore it is recommended that the behavior of stainless steel in heated brine be investigated.

This review identifies areas of uncertainty and/or knowledge gaps and outlines a set of laboratory experiments targeting these areas. Six tasks are proposed. Task 1 and 2 investigate the long-term corrosion rate of carbon steel in low and high-magnesium brines. Task 3 investigates the identity of the carbon steel corrosion products. Task 4 determines the chemical environment that the stainless steel will experience due to the corrosion of the overlying carbon steel. Task 5 determines the corrosion rates of stainless steels within the environments identified in Task 4. Finally, Task 6 investigates the identity of the stainless steel corrosion products.

CONTENTS

FIGURES

TABLES

USED FUEL DISPOSITION CAMPAIGN
Test Plan for Investigation of Material Interactions in Heated Salt
November 20, 2012

x

ACRONYMS, ABREVIATIONS, UNITS

A   ampere (a unit of electric current)
ACS   American Chemical Society
AISI   American Iron and Steel Institute
ASTM   American Society for Testing and Materials
atm   atmosphere (a unit of pressure)
B   boron
Brine A   A standard high-magnesium brine proposed by Molecke (1983)
Brine 3   A high-NaCl brine used by the Germans as reported by Kursten et al. (2004)
BSC   Bechtel SAIC Co. LLC
Ca   calcium
cc   cubic centimeter
CCP   cyclic potentiodynamic polarization
Cl   chlorine
cm   centimeter
DFT   density functional theory
DOE   United States Department of Energy
E_a activation energy
EDS   Energy Dispersive Spectroscopy
E-ERDA-6   equilibrated ERDA-6, ERDA-6 brine equilibrated with MgO
ERDA-6   Energy Research and Development Administration (WIPP Well) 6, Synthetic
             Castile Formation brine
E-GWB   equilibrated Generic Weep Brine, equilibrated with MgO
FCT   Fuel Cycle Technology
Fe   iron
g   gram
GWB   Generic Weep Brine, a synthetic Salado Formation brine
H   hydrogen
HER   hydrogen evolution reaction
ISO   International Organization for Standardization
K   potassium
kcal   kilocalorie
kJ   kilojoules
L   liter of solution
M   molar concentration (mol/L)
m   meter
M&TE   measuring and test equipment
Mg   magnesium
mg   milligram

MIC	microbiologically influenced corrosion
mM	milli molar
mm	millimeter
μm	micrometer
mol	mole
Na	sodium
NIST	National Institute of Standards and Technology
O	oxygen
ORR	oxygen reduction reaction
PA	Performance Assessment
PBB1	Permian Basin Brine Number 1. A high-NaCl brine used by Westerman et al. (1986, 1988)
PBB2	A high-NaCl brine used by Westerman et al. (1986, 1988)
PBB3	A high-Mg brine used by Westerman et al. (1986, 1988)
pcH	the negative log of the hydrogen ion concentration
pH	the negative log of the hydrogen ion activity
ppb	part per billion
ppm	parts per million
QA	Quality Assurance
Q-brine	(Brine 1) A high-Mg brine used by the Germans as reported by Kursten et al. (2004)
S	sulfur
s	second
SS	stainless steel
SEM	Scanning Electron Microscopy
SNL	Sandia National Laboratories
SOP	Standard Operating Procedure
TSPA	Total System Performance Assessment
TWP	technical work plan
UNS	Unified Numbering System
U.S.	United States
V	vanadium
V	volt
VASP	Vienna ab initio simulation package
WIPP	Waste Isolation Pilot Plant
wt%	weight percent
XRD	X-Ray Diffractometer

USED FUEL DISPOSITION CAMPAIGN

TEST PLAN FOR INVESTIGATION OF MATERIAL INTERACTIONS IN HEATED SALT

1.   INTRODUCTION

In March of 2012, the U.S. Department of Energy (DOE) offices of Nuclear Energy and Environmental Management issued a joint study plan outlining the technical objectives and science-based scope of work for the study of salt geologic media for disposal of DOE-owned and civilian high-level waste and used nuclear fuel. This test plan fulfills Task 3.5, "Test Plan for Investigation of Material Interactions in Heated Salt". As directed in the study plan, this test plan focuses on the corrosion of common materials used in waste disposal operations and the resulting corrosion products. This information is needed for the total system performance assessment (TSPA) model, which is the subject of Task 4.2. The ultimate goal of this task is to provide inputs needed by the TSPA model on the effects of corrosion of waste package materials on repository performance. The main effects of corrosion are the consumption of brine, the production of H_2 gas, and control of the repository chemistry—specifically, the reduction-oxidation conditions and the pH. The parameters needed by TSPA include the corrosion rates and the chemical control by the corrosion products.

The TSPA model is being developed for a "generic" salt repository, with the exact location or engineering design unspecified. However, a reference case including a concept of operations has been developed to provide enough detail on repository layout, emplacement mode for the waste, and selection of engineered materials for a TSPA model to be constructed. This reference case is outlined in the "TSPA Model Development and Sensitivity Analysis of Processes Affecting Performance of a Salt Repository for Disposal of Heat-Generating Nuclear Waste (Sevougian et al., 2012).   The reference case is for a repository within a bedded salt formation whose top is at depths of 1000 to 3500 feet (305 m to 1067 m), although a domal salt formation is not ruled out. In this concept of operations, minimal ground support, tunnel liners, or steel sets will be used in the emplacement drifts, as their structures could delay or prevent the desired encapsulation of the waste as the emplacement drifts close due to salt creep. This encapsulation is a key feature of a repository in salt, and it removes the requirement for long-term integrity of the waste package. The reference waste package consists of thin-walled (10 to 20 mm) stainless steel canisters surrounded by thick-walled carbon steel overpacks, both sealed with welded closures. A variety of stainless steels have been proposed, including type 304 and 316. The overpack will be designed to resist package breach from crushing or buckling for at least 300 years, the time period for possible waste retrieval. A preliminary overpack thickness of 7.5 cm is selected. The waste packages will be emplaced on the floor of emplacement drifts or in alcoves to the side of the drifts and covered with a crushed salt backfill. This backfill will have an emplacement porosity of about 35%, but will consolidate within a few decades as the drifts close due to creep of the host salt formation. Within about 300 years the backfill will attain a low permeability on

USED FUEL DISPOSITION CAMPAIGN
Test Plan for Investigation of Material Interactions in Heated Salt
November 20, 2012

2

the order of 10^{-17} m^2 or less. A temperature limit of 200℃ is placed on the interface between the waste packages and the salt.

Scope

The scope of this test plan is to fill data gaps in the corrosion rate data of waste package steels in a closed salt repository and to identify corrosion products. If brine is limited in the repository, the corrosion rates will drop until the water consumption rate matches the water influx rate at the waste package surface. Under these circumstances, it is not necessary to know the steady state corrosion rate in an unlimited quantity of brine, as the corrosion rate will be determined by the rate of brine influx. The rate of brine migration toward heated waste packages, however, is beyond the scope of this test plan, but is addressed as part of Task 3.4 "Brine Migration Experimental Studies", and will depend upon the salt deposit chosen for the repository (bedded or domal). Since it is not known at this time whether the corrosion of the waste package will be brine-limited, it is necessary to obtain the corrosion rates for conditions were brine is not limited. This test plan focuses on corrosion rates in the presence of an unlimited volume of brine..

Assumptions

This test plan adopts the assumptions from the reference case (Sevougian et al., 2012) as follows: 1) the repository will be located in a domal or bedded salt formation, 2) the waste package will be backfilled with mined crushed salt, and 3) the waste package will consist of a stainless steel canister with a carbon steel overpack. In addition, the assumption of unlimited brine is made for the purposes of this test plan. The impact of these assumptions are: 1) The fluids contacting the waste packages will be saturated brines, 2) The waste package surface will be contacted by consolidating salt, 3) the materials to test will be carbon and stainless steel, and 4) the effects of brine availability on corrosion rates will not be investigated under this test plan. If any of these assumptions change, the test plan would have to be re-evaluated.

Organization

This test plan is organized into two main sections, a literature review and an experimental section. The literature review covers: 1) the ranges in brine compositions applicable to a generic salt repository, 2) corrosion rates and corrosion products for carbon steels in various brine chemistries, and 3) corrosion rates and corrosion products for stainless steels in various brine chemistries. Gaps in the literature are identified. The experimental section outlines the tests to fill the data gaps.

2.   LITERATURE REVIEW

In order to determine corrosion rates and corrosion products, two things must be known with some specificity: environment and material. A general description of these has been provided in the Salt Disposal Reference Case as a bedded or domal salt repository and carbon and stainless steels. A literature review of the potential repository environments, and the corrosion rates and corrosion products of carbon and stainless steel in these environments are provided in Sections 2.1 through 2.3.

2.1   Salt Repository Environment

Hansen and Leigh (2011) describe the salt formations in the U.S., which are often categorized as "bedded" or "domal." Bedded formations of salt are found in layers interspersed with materials such as anhydrite, shale, dolomite, and other salts such as potassium chloride. Domal formations (i.e., salt domes) form from salt beds when the density of the salt is less than that of surrounding sediment. Under such conditions, the salt has a tendency to move slowly upward toward the surface. As the buoyant salt moves upward, it deforms plastically into mushroom-shaped diapirs and many other cylindrical and anticlinal shapes. The top of some domal salt can be near surface, while the root may extend to a great depth.

Bryan et al. (2011) summarized the brine content of salt formations as follows: "*The water (brine) content of domal salt is on the order of thousandths, hundredths, or tenths of a wt. %; that of bedded salt is on the order of tenths to a few wt% (Roedder and Belkin, 1979; Jockwer, 1981; Knauth and Kumar, 1981; Roedder and Bassett, 1981; Rothfuchs, 1986; De Las Cuevas and Pueyo, 1995). These brines are present within individual salt crystals (i.e., intragranular brine or fluid inclusions), along the boundaries between salt crystals (intergranular brine), and as structural water in hydrous minerals such as clay minerals and the evaporite minerals gypsum ($CaSO_4 \cdot 2H_2O$), and polyhalite $K_2MgCa_2(SO_4)_4 \cdot 2H_2O$).*"

The brines that may interact with the waste package can come either from the immediate surrounding salt formation, or from outside the repository horizon. The first case involves migration of the intergranular or intragranular brine or water released from hydrated minerals toward the hot waste packages. These brines migrate through halite, sylvite and Mg-containing hydrous minerals (e.g. bischofite, carnallite and polyhalite) and thus are saturated brines with high-Na-Mg-K-Cl content (Molecke, 1983). The amount of this brine is limited by the water content of the host rock salt formation. The second case is much less likely, but can deliver larger quantities of brine to the repository.   Originally fresher water may migrate to the repository along a defective borehole seal plug, along a clay seam, fracture paths, impurity bed. As the water migrates toward the repository, it will dissolve salts along the way and will become saturated with NaCl. Depending on the purity of the salts intersected, and the volume of brine involved, this brine may be a high-NaCl brine. In addition, if the drillers intercept both the repository and an underlying pressurized brine pocket, the amounts of brine delivered to the waste packages near the drill hole can be very large. If the composition of pocket brine is that which would be obtained by dissolving the host rock salt to saturation, this too could be a high-NaCl brine.

Table 2-1 summarizes some brine compositions found at bedded salt deposits in the U.S. along with the composition of seawater. There is quite a range of compositions with concentrations of sodium up to 168,000 mg/l, magnesium up to 54,000 mg/l, potassium up to 63,000 mg/l, calcium up to 107,000 mg/l, sulfate up to 25,200 mg/l, and chloride up to 264,000 mg/l. These can be compared to 142,000 mg/l sodium and 218,000 mg/l chloride for a saturated NaCl solution at 20°C. The total cation concentration is not unlimited, so that as the concentration of other cations goes up, sodium concentration tends to go down. Chloride concentration goes up with the concentration of divalent cations.

Brines from the Delaware Basin within the Permian Basin have been extensively studied for the Waste Isolation Pilot Plant (WIPP) transuranic waste repository and some representative compositions are included in Table 2-2. The brines flowing from pockets below the repository horizon at the ERDA-6 and WIPP-12 wells are mainly NaCl brines, while the brines weeping into the repository from the host rock and brines from inclusions in the salt are lower in sodium but higher in magnesium, potassium, and chloride.

Table 2-1. Some U.S. Major Element Brine Compositions

	Description	Concentration (mg/l)						pH
		Na^+	Mg^{2+}	K^+	Ca^{2+}	SO_4^{2-}	Cl^-	
A	Seawater	10651	1272	380	400	884	18980	8.1
B	Permian Delaware (WIPP)	34800 - 140000	270 - 54000	3100 - 20400	120 - 490	14000 - 25200	160000 - 217200	6.4 - 7.8
C	Michigan Basin Devonian	12400 - 103000	3540 - 14600	440 - 19300	7390 - 107000	0 - 1130	120000 - 251000	3.5 - 6.2
D	Paradox Formation Moab Region	9800 - 25966	21000 - 47789	23400 - 41957	34000 - 65800	80 - 1800	29800 - 259106	4.8 - 6.0
E	Paradox Basin Mississippian Formation	132000 - 168000	324 - 9000	NR	288 - 14400	2160 - 8800	183600 - 264000	4.6 - 6.7
E	Paradox Basin Paradox Formation	26640 - 119880	5160 - 39480	25680 - 63000	6036 - 51240	306 - 5268	145080 - 260640	4.9 - 6.2

Notes: A Molecke, 1983
B See Table 2-2
C Wilson and Long, 1993
D DOE, 2007
E Garrett, 2004 summary of Mayhew and Heylmun, 1966 data.

Table 2-2. Brine Compositions in and Around the WIPP site

	Description	Concentration (mg/l)						pH
		Na^+	Mg^{2+}	K^+	Ca^{2+}	SO_4^{2-}	Cl^-	
A	ERDA-6 down hole	140000	270	4800	360	14000	180000	7.02
A	ERDA-6 flow	112000	450	3800	490	16000	170000	6.42
A	WIPP-12 down hole	140000	1400	3200	380	18000	180000	7.76
A	WIPP-12 flow	114000	1700	3100	410	17000	160000	7.17
B	Inclusion Group I	34800	54000	8400	120	21600	213600	NR
B	Inclusion Group II	69600	32400	12000	240	25200	200400	NR
B	Weeps	88800	25200	20400	360	14400	217200	NR

Notes: A Molecke, 1983
        B Stein and Krumhansl, 1988 Table 4. Values converted from parts per thousand
        assuming a brine density of 1.2 gm/cc.
        NR Not recorded

2.2   Corrosion of Carbon Steel

2.2.1   Background

Two types of corrosion processes can occur in the disposal rooms of a salt repository, namely oxic and anoxic corrosion processes. Shortly after emplacement of the repository seal systems, oxic conditions will be predominant. After the depletion of oxygen initially present by oxic corrosion reactions, anoxic corrosion of Fe-based materials will prevail and will produce hydrogen gas and consume water. Oxic corrosion will be brief on repository performance time scales, and will not significantly affect the water and gas balance of the system, so anoxic corrosion is the main focus of this test plan. However, oxic corrosion will occur, and it is included in the following discussion of the major reactions and mechanisms for corrosion of Fe-based materials in water and brines.

2.2.1.1   Corrosion of Iron in Water

Under oxic conditions, Fe-based materials exposed to molecular oxygen in the presence of pure water (as vapor or liquid phase) will corrode and form hydrated iron oxides and hydroxides via the reactions (Hoerle et al., 2004):

$$2\ Fe + O_2 + 2\ H_2O \rightarrow 2\ Fe(OH)_2. \tag{2-1}$$
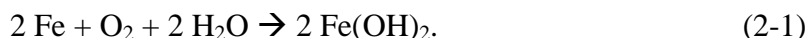
Further exposure of the iron(II) hydroxide produced in reaction 2-1 to molecular oxygen and water might result eventually in the formation of iron(III) hydroxide (ferrihydrite):

$$4\ Fe(OH)_2 + O_2 + 2\ H_2O \rightarrow\ 4\ Fe(OH)_3. \tag{2-2}$$

This product can undergo further dehydration via the reaction:

$$Fe(OH)_3 \rightarrow \quad FeOOH + H_2O, \quad\quad\quad (2\text{-}3)$$
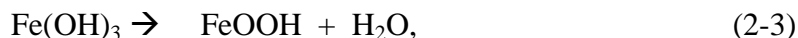
FeOOH generated in reaction 2-3 can be converted to Fe_2O_3 through the reaction:

$$2\ FeOOH \rightarrow Fe_2O_3 + H_2O. \quad\quad\quad (2\text{-}4)$$

Near the metal surface where oxygen is more limited, $Fe(OH)_2$ may partially oxidize to form the mixed valence oxide magnetite.

$$3\ Fe(OH)_2 + 2\ O_2 \rightarrow \ Fe_3O_4 + 3\ H_2O \quad\quad\quad (2\text{-}5)$$
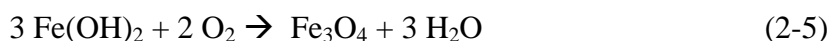
It should be noted that rust layers typically formed under oxic conditions are actually more complex than suggested by the previous reactions; rust layers are usually composed of several oxides and hydroxides, a subset of which is presented in Table 2-3 (Hoerle et al., 2004).

Table 2-3. Some of the Oxides and Hydroxides Found in Rust Layers

Composition	Name	Crystal System
Fe_3O_4	Magnetite	Cubic (spinel)
γ-Fe_2O_3	Maghemite	Cubic (spinel)
α-FeOOH	Goethite	Orthorhombic
γ-FeOOH	Lepidocrocite	Orthorhombic
β-FeOOH	Akaganeite	Tetragonal
γ-Fe·OH·OH	Reduced lepidocrocite	Orthorhombic
$Fe(OH)_2$	Ferrous hydroxide	Hexagonal

Oxic corrosion of Fe-based materials occurs by a combination of two coupled reactions: an anodic reaction which is oxidation of the Fe to Fe^{+2} or Fe^{+3} and a cathodic reaction. The operative cathodic reaction or reactions will depend on the availability of dissolved oxygen and the pH of the environment and can include oxygen reduction or water reduction.

Under oxic conditions, the dominant cathodic reaction is generally the oxygen reduction reaction (ORR), (Equation 2-6) where dissolved oxygen in the solution is reduced. This is a mass-transport controlled reaction, where the maximum rate at which it can progress is limited by the ability of oxygen to diffuse to the metal surface. As such, increasing the temperature (and hence diffusivity) or oxygen concentration in the bulk will increase the maximum cathodic reaction rate which can be supported at the metal surface.

$$O_2 + 4e^- \rightarrow 2\ O^{-2} \quad\quad\quad (2\text{-}6)$$

Under anoxic conditions, the limiting reaction rate of the ORR becomes exceedingly slow. If it is the only viable cathodic reaction, the anodic reaction rate (i.e., iron oxidation) must also

decrease. However, the hydrogen evolution reaction (HER) can become thermodynamically viable in certain conditions, and high dissolution rates may still be supported as the HER is a charge transfer controlled reaction.

At neutral and alkaline pH levels, the reversible potential for the hydrogen evolution reaction (HER), reactions 2-7 or 2-8, is sufficiently low that it is not a viable cathodic reaction to support iron oxidation. As the pH is reduced, the reversible potential moves further in the positive direction, and may eventually become a viable cathodic reaction (i.e., the reversible potential is sufficiently anodic (i.e., more positive) when compared to the reversible potential for iron oxidation, that it becomes possible to support iron oxidation from a thermodynamic point of view). Unlike oxygen reduction, the hydrogen evolution reaction (HER) (or water reduction, reaction 2-8) is a charge transfer controlled process. As such, it is not controlled by mass transport processes, and can support very high reaction rates.

$$2\,H^+ + 2e^- \rightarrow H_2 \qquad\qquad (2\text{-}7)$$
$$2\,H_2O + 2\,e^- \rightarrow 2\,OH^- + H_2 \qquad\qquad (2\text{-}8)$$
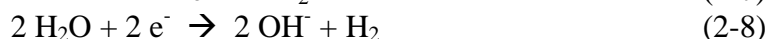
As the corrosion process progresses, iron ions will be driven into solution, where they may hydrolyze. Hydrolysis of the iron cations (equations 2-9 through 2-13) will decrease the pH, increasing the aggressiveness of the solution and if the pH is sufficiently low, making the HER a viable cathodic reaction. Both ferrous (Fe^{2+}) and ferric (Fe^{3+}) ions may hydrolyze.

$$Fe^{2+} + H_2O \leftrightarrow Fe(OH)^+ + H^+ \qquad\qquad (2\text{-}9)$$
$$Fe(OH)^+ + H_2O \leftrightarrow Fe(OH)_2 + H^+ \qquad\qquad (2\text{-}10)$$
$$Fe^{3+} + H_2O \leftrightarrow Fe(OH)^{+2} + H^+ \qquad\qquad (2\text{-}11)$$
$$Fe(OH)^{+2} + H_2O \leftrightarrow Fe(OH)_2^+ + H^+ \qquad\qquad (2\text{-}12)$$
$$Fe(OH)_2^+ + H_2O \leftrightarrow Fe(OH)_3 + H^+ \qquad\qquad (2\text{-}13)$$

Low pH can also increase the stability of Fe^{2+} and Fe^{3+} in solution and thus prevent stifling of the anodic reaction by precipitating phases. The stability of ions in solution and solid corrosion products are succinctly represented in potential-pH diagrams often referred to as Pourbaix diagrams (Pourbaix, 1974).

In general, the cathodic reaction, anodic reaction, and the mass transport (i.e., diffusion) of cations and/or anions through the corrosion product layer, are accelerated by increasing the temperature. Furthermore, the thermodynamic stabilities of dissolved and solid species change with temperature. As a result, the corrosion products which are stable will change. This can have an impact on the anodic reactions which are thermodynamically viable on the metal surface, as well as result in the formation of oxidation product layers (i.e., corrosion products) on the surface which can hinder both the anodic and cathodic reactions.

The temperature dependence of the general corrosion rate can often be described using the Arrhenius equation

$$Corrosion\ Rate = Ae^{-\frac{E_a}{RT}} \qquad\qquad (2\text{-}14)$$

where A is a prefactor, E_a the activation energy, T is the temperature in Kelvin. Both the prefactor term and the activation energy are functions of the factors influencing the rate limiting reaction.

2.2.1.2   *Corrosion of Iron in Chloride-Rich Brine*

The behavior of carbon steels in chloride-rich brine is markedly different than in high purity water as discussed in the preceding sections, both in terms of thermodynamic and kinetic considerations. The thermodynamic differences are illustrated by comparing the E-pH diagram for the Fe-Cl-H_2O system. MacDonald et al. (1979) produced such diagrams for Fe, Ni, Cr, and Ti in high salinity geothermal brines at 25^{0}C and 250^{0}C. While the identity and stability of dissolved species remain controversial, these diagrams are illustrative. The 25^{0}C diagram for Fe shows that under oxidizing conditions the stable dissolved species are $FeCl_2^+$ at pH values below 4 and $Fe(OH)_3$ above. Under reducing conditions, the stable species are Fe^{2+} at pH values below about 9.5 and $Fe(OH)_3$ above. At intermediate redox conditions the position of stability boundary between Fe^{2+} and $Fe(OH)_3$ depends on the potential, with a diagonal line from 9.5 pH at low potential to 4 at high potential. Thus when iron is corroding in oxic brines that start at neutral pH values, reactions 2-11 through 2-13 will occur driving the pH down until Fe^{2+} or $FeCl_2^+$ are the stable species. Only at low potentials and pH values above 9.5 will reaction 2-9 drive down the pH. The stability field for the solid phase Fe_2O_3 overlaps the stability field for dissolved $Fe(OH)_3$ and there are no iron oxide or oxyhydroxide solid phases stable at the lower pH and potential values. MacDonald et al. (1979) did not include the more soluble solid iron hydroxide or chloride phases in their calculations, so it is not clear at what high Fe^{2+} concentrations such solids might form. However, until there are very high Fe^{2+} concentrations, there are no solid phases to slow down the corrosion reaction when it is occurring at low pH. The only other solid phase in the diagram by MacDonald et al. (1979), Fe_3O_4, only occurs at low potentials, near the line for reduction of water to one atmosphere (atm) H_2 gas, and above pH values of about 8.

The potential-pH diagram for Fe at 250^{0}C by MacDonald et al. (1979) is quite different than the one for 25^{0}C (discussed above), with the stability fields for dissolved and solid species shifting to lower pH values at higher temperatures. At high temperatures and medium to high potentials there are three stable dissolved Fe(III) species: $FeCl_{3(aq)}$ up to a pH value of about 3, $Fe(OH)_{3(aq)}$ between 3 and 9 and $Fe(OH)_4^-$ above a pH value of 9. Thus corrosion of iron under typical brine conditions at high temperature, reactions 2-11 through 2-13 are active, reducing the pH to values lower than achieved at low temperatures. Only at low potentials, near the line for reduction of water to one atmosphere H_2 gas, are dissolved Fe(II) species stable: Fe^{2+} up to a pH value of about 3, $Fe(OH)^+$ between 3 and 4.5, $Fe(OH)_{2(aq)}$ between 4.5 and 10, and $HFeO_2^-$ above a pH value of 10. Thus at low potentials and high temperatures, reactions 2-9 and 2-10 will cause a drop in the pH, different from low temperatures and neutral pH values where neither of these reactions occur. For solids, the stability fields for Fe_2O_3 and Fe_3O_4 are significantly extended to the lower pH values of between 2 and 3.

2.2.2   Corrosion Rates of Carbon Steels in Salt Repositories

In salt repositories, the time period over which oxic conditions will exist is relatively short due to oxygen consumption by the corrosion reactions and the sealed nature of the repository after closure. Oxic corrosion has a minimal impact on the gas and water content of the repository, with the consumption of O_2 gas within the trapped air occurring soon after closure.   Anoxic corrosion, however, consumes water and generates H_2 gas in significant amounts, and thus affects the water and gas flow within the repository. This review focuses on anoxic corrosion.

Anoxic corrosion rates of clean surfaces of carbon steel under humid conditions are exceedingly low compared to the rates of surfaces contacted by brines (Telander and Westerman, 1993 and 1997, Roselle, 2009), however clean surfaces will not be present in a repository because the waste packages will be backfilled with mined salt. During the emplacement period, evaporation will occur and the relative humidity in the salt around the waste packages will decrease below that typical in salt formations of about 75%. However after closure, as brine migrates into the repository and the pressures rise, relative humidities of 75% will be reinstated and deliquescence of the more hygroscopic constituents of salt on the surface of the waste package will occur. For example $MgCl_2$ deliquesces at about 30% relative humidity (Mintz et al., 2012). Thus thin brine films may be present on the waste package surfaces even in the absence of significant brine in the immediate vicinity. As previously mentioned, transport of brine toward the waste package is covered under another test plan. Therefore this literature review focuses on corrosion of carbon steels under inundated conditions.

Internationally, carbon steel had been proposed as a corrosion allowance material to use for overpacks in salt repositories. Carbon steel undergoes mainly general corrosion in brines, and does not undergo localized corrosion, and thus its behavior is theoretically relatively predictable. A number of studies have been performed to elucidate the behavior of carbon steels in anoxic brines or salt-brine mixtures, including those performed for a German repository (Kursten et al., 2004), the U.S. transuranic waste repository at the WIPP (Telander and Westerman, 1993 and 1997), (Roselle, 2009), and for generic U.S. salt repositories (Westerman et al., 1986 and 1988). These studies have been reviewed by Bryan et al. (2011), and highlights of the information from Bryan et al. (2011) and the original reports are provided here. Corrosion rates for inundated conditions are presented, followed by discussions of the data, and the effects on corrosion rates of the alloy, sample treatment including welds, brine composition, salt-brine ratios, temperature, test duration, H_2 pressure, pH, and gamma radiation.

2.2.2.1   Corrosion Rates

Corrosion rates measured in high-magnesium brines are provided in Table 2-4, and those measured in predominantly NaCl brines (low-magnesium brines) are provided in Table 2-5. The compositions of the brines and alloys used in the tests are provided in Tables 2-6 and 2-7. For comparison purposes, Arrhenius-type plots showing the natural logarithm of the minimum and maximum corrosion rates for each condition plotted against the reciprocal of the temperature in Kelvin are provided in Figures 2-1 and 2-2. If the Arrhenius equation (Equation 2-14) is

applicable to these data, the slopes of the data in these figures gives the activation energy of the corrosion process (E_a) divided by the gas constant (R).

It should be noted that for many of the studies on carbon steels in brines, while the corrosion rates are similar in magnitude, there is considerable variability, even within a single set of results. This is demonstrated in Figures 2-1 and 2-2, where scatter in the data in excess of 1.5 orders of magnitude is observed within a single environment/temperature combination. However some of the scatter is the result of plotting the results from all time periods reported. For the low-Mg brines, in some cases the corrosion rates decreased with time, and the initial corrosion rates are higher than the long-term rates. If the initial rates are discounted, the maximum corrosion rates are not quite as high, however and the spread remains over a factor of 5 for much of the data. When comparing the results obtained over differing temperatures and environmental conditions, the inherent uncertainties associated with each data set must be considered.

Table 2-4. Corrosion Rates of Carbon Steels in High-Magnesium Brines

| | | | | Corrosion Rate | | |
| | | | | Mean or least squares slope | Minimum | Maximum |
Reference	Brine	Material	°C	µm/year	µm/year	µm/year
A	E-GWB	A1008	26	0.139	0.06	0.233
B	"Brine A"	A366, A570	30	0.82	0.85	2.6
C	PBB3	A216	90	40	18	68
C	PBB3	A216	150	910	690	1540
C	PBB3	A216	200	3300	1570	7080
D (a)	Q Brine	TStE 355	90	69.7	67.9	71.5
D (a)	Q Brine	TStE 355	150	227	210.18	243.42
D (a)	Q Brine	TStE 355	170	199	184.4	214.4
D (a)	Q Brine	TStE 355	200	463	429.2	496.4
E (a)	Q Brine	TStE 355	150	47.1	44.6	49.6

(a) The minimum reported here is the average minus the error, and the maximum is the average plus the error

A   Roselle, 2009, 2010, 2011a, 2011b, immersed, 6, 12, 18 and 24 month data

B   Telander and Westerman, 1993, App. B-1, immersed 3-24 month data

C   Westerman et al., 1988, App. A.1, immersed, 1,3 and 6 month data, as cast, normalized, and welded samples.

D   Kursten et al., 2004, Tables 4-5 and 4-6, immersed, 5ml/cm2, 60-322 days

E   Smailos et al., 2003, Table 1, immersed, 2 ml/cm2, 100-600 days

Table 2-5. Corrosion Rates of Carbon Steels in Low-Magnesium Brines

				Corrosion Rate		
				Mean or least squares fit	Minimum	Maximum
Reference	**Brine**	**Material**	**°C**	**µm/year**	**µm/year**	**µm/year**
A	E-ERDA-6	A1008	26	0.243	0.012	0.465
B	"ERDA-6"	A366, A570	30	1.37	0.86	3.19
C	PBB1	A216	90	6	2.8	9.2
C	PBB1	A216	150	13.3	4.3	33
C	PBB1	A216	200	8.1	6.3	68
C	PBB1	A216	90	1.7	0.92	3.9
C	PBB1	A216	150	9.8	1.9	20.8
C	PBB1	A216	200	33.4	18	108
D (a)	Brine 3	TStE 355	90	5.1	2.9	7.3
D (a)	Brine 3	TStE 355	170	46	38.7	53.3
D (a)	Brine 3	TStE 355	200	18.3	14.7	21.9
D (a)	Brine 3	TStE 355	150	35.7	31.24	40.16
E (a)	Brine 3	TStE 355	150	15.3	14.3	16.3
F (a)	PBB2	A216	150	14.6	13.89	15.31
F (a)	PBB2	Fe	150	9.8	8.69	10.91
F (a)	PBB2	AISI 1025	150	8.6	7.77	9.43
F (a)	PBB2	A27 normalized	150	7.1	6.22	7.98
F (a)	PBB2	A536-77	150	6.9	5.92	7.88
F (a)	PBB2	A27 cast	150	5.3	4.48	6.12

(a) The minimum reported here is the average minus the error, and the maximum is the average plus the error

A Roselle, 2009, 2010, 2011a, 2011b, immersed, 6, 12, 18 and 24 month data

B Telander and Westerman, 1997, App. B-3, immersed, 10 month data

C Westerman et al., 1988, App. L.1, brine in salt, 20% and 5% H_2O, 3 and 6 month data, as cast, normalized, and welded samples.

D Kursten et al., 2004, Tables 4-5 and 4-6, immersed, 5ml/cm2, 60-322 days

E Smailos et al., 2004, Table 3.3, immersed, 2 ml/cm2, 100-600 days

F Westerman et al., 1986, Table 4, immersed, 6 month data

Table 2-6. Compositions of Test Brines (mg/L)

Note	Brine	Na^+	Mg^{2+}	K^+	Ca^{2+}	SO_4^{2-}	Cl^-	C	pH
				High Magnesium					
A	PBB3	23,000	60,000	11,000	18,700	250	240,000	NR	NR
B	"Brine A"	39,400	34,700	29,900	560	4,130	188,300	680	7.4
C	E-GWB	101,000	13,600	19,200	438	17,700	197,000	NR	7.6
D	Q Brine (Brine 1)	6,500	85,000	29,000	NR	13,000	270,000	NR	4.3-4.6
				Low Magnesium					
A	PBB1	123,000	134	39	1,560	3,200	191,000	30	7.055[*]
A	PBB2	123,000	122	39	1,110	1,910	191,000	23	NR
E	E-ERDA-6	123,000	2,600	3,770	454	16,200	188,000	NR	7.96
F	"ERDA-6"	113,000	-	3,770	-	16,100	164,000	NR	6.15
D	Brine 3	122,000	390	619	740	4,800	189,000	NR	6.5-6.9

Notes:
A   Westerman et al., 1988, Table 4.3
B   Telander and Westerman, 1993, Table 5-3 "Brine A" is in quotes because the brine is not quite the same as Brine A by Molecke, 1983.
C   Roselle, 2009, Table 2-3, converted from molal using a brine density of 1.23. E-GWB (equilibrated GWB) is based on calculations of GWB brine (Snider, 2003) equilibrated with MgO by Brush, 2005.
D   Kursten et al., 2004, Table 4-3, converted from wt% assuming brine average density of 1.2 mg/l.
E   Roselle, 2009, Table 2-3, converted from molal using a brine density of 1.22. E-ERDA-6 (equilibrated ERDA-6) is based on calculations of ERDA-6 brine (Popielak et al., 1983) equilibrated with MgO by Brush, 2005.
F   Telander and Westerman, 1997, Table 5-5, "ERDA-6" is in quotes because the brine is not quite the same as ERDA-6 by Molecke, 1983.
NR   Not recorded
*   Also known as ONWI Composite Permian P. pH from Molecke, 1983, Table 1.

Table 2-7. Compositions of Steels Used in Tests (weight percent)

Ref.	Steel	C	Si	P	S	Cr	Mn	Ni	Cu	All Other	Fe
A	A216 lot 1	0.23	0.45	0.018	0.018	0.41	0.71	0.23	0.14		Balance
A	A216 lot 2	0.16	0.58	0.014	0.014	0.13	0.6	0.08	0.08		Balance
A	Weld wire	0.04	0.42	0.015	0.012		1.48				Balance
B	TStE 355	0.17	0.44				1.49				Balance
C	A366, lot J	0.06	0.08	0.015	0.012		0.3		0.015		Balance
C	A366, lot K	0.05	0.07	0.015	0.009		0.30		0.020		Balance
C	A570, lot L	0.13	0.11	0.017	0.015		0.77		0.015		Balance
C	A570, lot M	0.13	0.10	0.020	0.015		0.75		0.040		Balance
D	A1008	0.05	0.01	0.006	0.005	0.04	0.01	0.04	0.11	0.06	Balance
E	Fe	0.018	0.01	0.002	0.003	0.01	0.05	0.01		0.01	Balance
E	AISI 1025	0.07	0.03	0.015	0.021		0.40				Balance
E	A27	0.245	0.59	0.016	0.018	0.43	0.69	0.20		0.04	Balance
E	A536-77	3.53	2.51	0.05	0.004		0.31				Balance

A   Westerman et al., 1988, Table 4.1

B   Kursten et al., 2004, Table 4-1

C   Telander and Westerman, 1997, Table 5-1

D   Roselle, 2009, Table 2-1, other elements were Al 0.026, Ca 0.001, Mo 0.010, N 0.009, Nb 0.003, Sn 0.007, Ti 0.002 and V 0.002

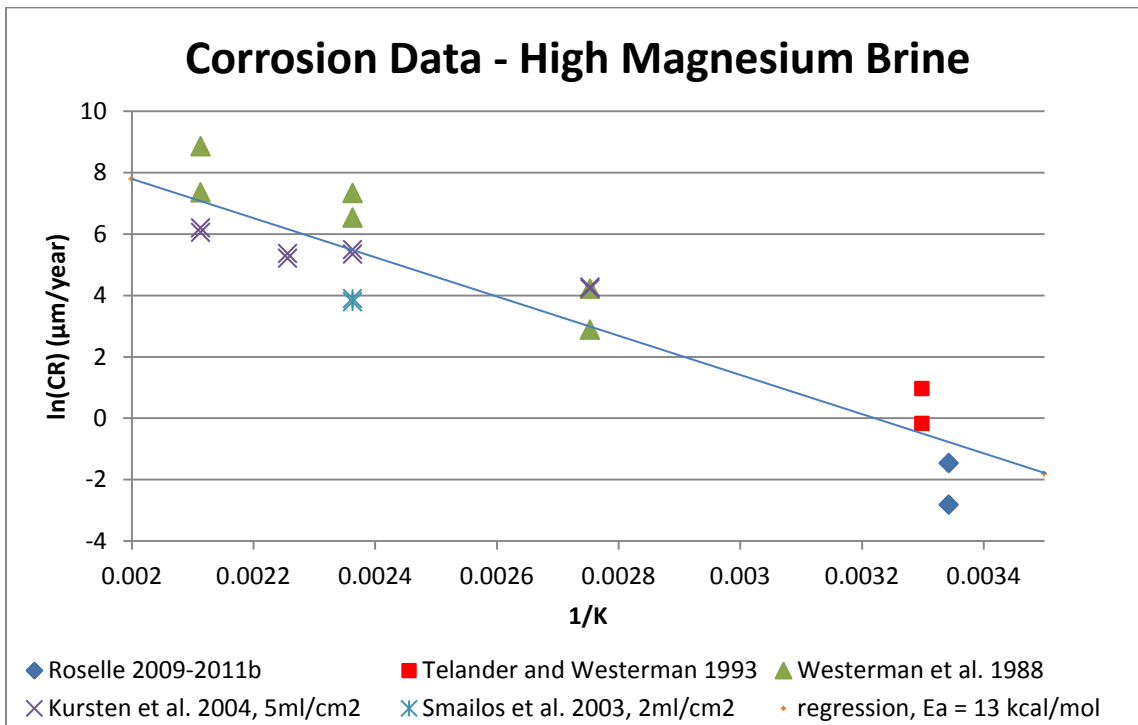E   Westerman et al., 1986, Table 1, the other element was Mo

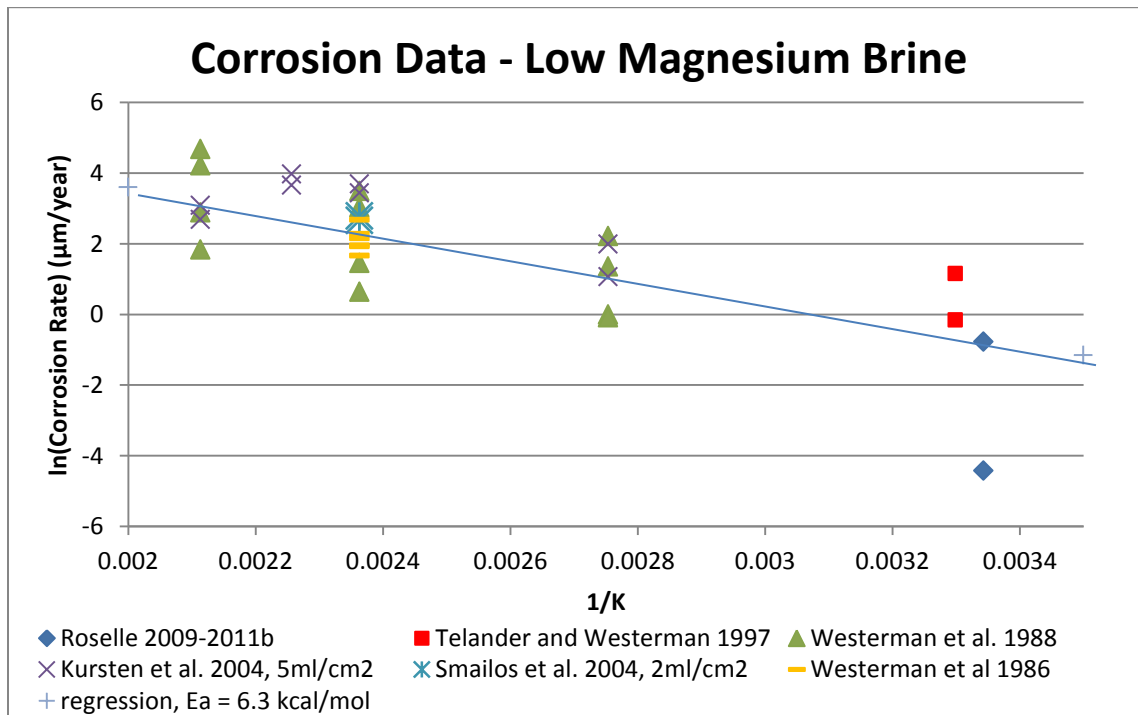Figure 2-1. Corrosion Data for Carbon Steels in High Magnesium Brines

Figure 2-2. Corrosion Data for Carbon Steels in Low Magnesium Brines

2.2.2.2   *Discussion of the Data Acquisition*

The treatment of the weight loss data to obtain the corrosion rates in the tables merits discussion. For weight loss testing, the dimensions and mass of each coupon are carefully documented prior to the initiation of the test. Upon completion of the test, the samples are cleaned of any residual corrosion product, and weighed again. The average depth of attack can then be calculated as $\Delta W/(SA*\rho)$, where ΔW is the weight change, SA is the surface area of the coupon (calculated from the initial dimensional data), and ρ is the density of the material. This average depth of attack can be turned into a corrosion rate by dividing by the time period of the test. Achieving a high level of accuracy with the weight loss method requires that extreme care be taken when measuring the dimensions of the coupons and the mass of the coupons prior to, and upon completion of the test. Furthermore, the geometry of the test specimens should be as uniform and with as high a surface area as can be reasonably achieved. In addition, the use of well defined standards for both mass and length, as well as the implementation of National Institute of Standards and Technology (NIST) single- or double-substitution weight measurement methods can significantly improve the quality of the data. As with the measurement techniques employed in weight loss testing, the manner in which the coupons are prepared prior to and following corrosion testing can have a profound impact on the accuracy and repeatability of the results. In order to measure an accurate weight loss, it is imperative that all of the corrosion products be removed from the surface. This requires the application of a test procedure which not only removes the corrosion product, but is also capable of taking into account any base metal which is removed in the process. Such procedures are outlined in American Society for Testing and Materials (ASTM) G1 and elsewhere (e.g., ISO 8407). Carbon steel and stainless steels are expected to corrode relatively rapidly in concentrated brines; anticipated weight changes are relatively large. Hence, corrosion rate measurements for these experiments should not tax the precision of the technique, as measurements of other, more passive metals sometimes does.

It should be noted that the weight-loss method provides a time-averaged corrosion rate, rather than an instantaneous corrosion rate. This is important, as for many situations the corrosion rate will initially be high, and will then decay down to some steady state value over time. As a result, time averaged corrosion rates can overestimate the instantaneous corrosion rates for times up to, and depending on the magnitude of the corrosion rate, considerably beyond when the steady state corrosion rate is reached. To obtain the instantaneous corrosion rate via weight change data, data is needed from many time intervals. The slope of the depth of attack vs. time at any specific time represents the instantaneous corrosion rate at that time.

For corrosion allowance materials as well as corrosion resistant materials, there can be considerable experimental variability. Consider the data from Westerman et al., 1988 for carbon steel samples in PBB1 brine with an excess of salt with 20% H_2O at 150°C presented in Figure 2-3. As can be seen in the data, there is considerable uncertainty at each time interval. As a result, care must be taken in interpreting the data. From the data, the average corrosion rate at 3 months is 19±6 µm/yr and at 6 months, is 16±6 µm/yr, suggesting that the corrosion rate is decreasing with time, however not significantly so.

Another example from Westerman et al. (1988) is presented in Figure 2-4, this time for a lower temperature. In this example, the average depth of attack is constant as a function of time – as a result, if the average corrosion rate were calculated for each time interval, it would appear that the corrosion rate was decreasing, but measureable, at each time interval. However, looking at the slope of the depth of attack vs. time plot, it can be seen that the corrosion rate has clearly decayed to below the resolution of the experimental technique. In all likelihood, the corrosion rate was initially high, but then slowed significantly. This reduction in rate could be due to precipitation of a passivating corrosion product layer, or the limitation of mass transport to the metal surface due to the precipitation of a salt film. Whatever the reason, using the average corrosion rate calculated as discussed above at longer time intervals would clearly grossly overestimate the instantaneous corrosion rate at that time.

In Tables 2-4 and 2-5, the values reported are either the mean of the time-averaged corrosion rate data, or the slope of a least squares fit to the penetration depth versus time data. The slope of a least squares fit to the data was used when data is reported for more than one period and when such a treatment is considered reasonable. The data in Figure 2-3 is an example where the slope is reported. Note that the slope of 13.333 is one standard deviation lower than the mean of the 3 month data and one half of a standard deviation lower than the mean of the 6 month data. However, when data from only one time period is available or when the slope does not make physical sense, the mean of the time-averaged corrosion rate data is reported in Tables 2-4 and 2-5. The data shown in Figure 2-4 is an example where the slope is not used. A negative slope is clearly not physical. In this case, the mean of the 6-month corrosion data is reported as an upper limit for the corrosion rate.

The scatter in the data may be due to variations in the general corrosion rate over the surface of the specimens. In 1988, Westerman et al. did not comment on the uniformity of the general corrosion observed, but in 1986 they describe the corrosion attack to be "*reasonably uniform … there was no evidence of non-uniform attack progressing into the metal more than a tenth of a millimeter or so beyond the surface of the specimen.*"   Since the reported corrosion rates range from 0.92 to 108 μm/year, non-uniform attack of 100 μm could have a major impact on test reproducibility. It is important to note, however, that no evidence of pitting or crevice corrosion was observed in tests specifically designed to investigate them. The Westerman et al. (1988) general corrosion tests used as-cast, normalized, and welded coupons. Normalizing is a thermal processing procedure where the steel is heated into the austenite phase field and held to transform from ferrite+cementite to austenite. The material is then air cooled, and the resulting microstructure is a uniform ferrite+pearlite. Coupon dimensions were typically about 15 mm x 15 mm x 1.5 mm in dimension. However, little difference was seen between the as-cast, normalized, and welded corrosion rates in the tests in the PBB1 brine/salt mixture shown in Figures 2-3 and 2-4. In these tests, a black corrosion product, identified as either magnetite (Fe_3O_4) or magnesioferrite ($MgFe_2O_4$) by X-Ray Diffractometer (XRD), coated the specimens.
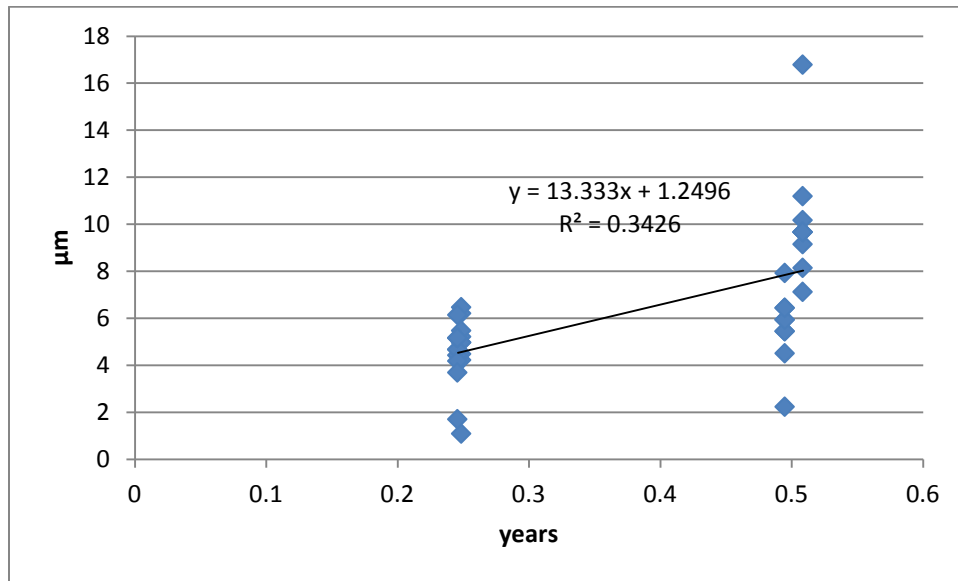
Source: Westerman et al., 1988 for PBB1 brine in salt with 20% H_2O and 150⁰C

Figure 2-3. Corrosion Penetration Depth versus Time - Example 1
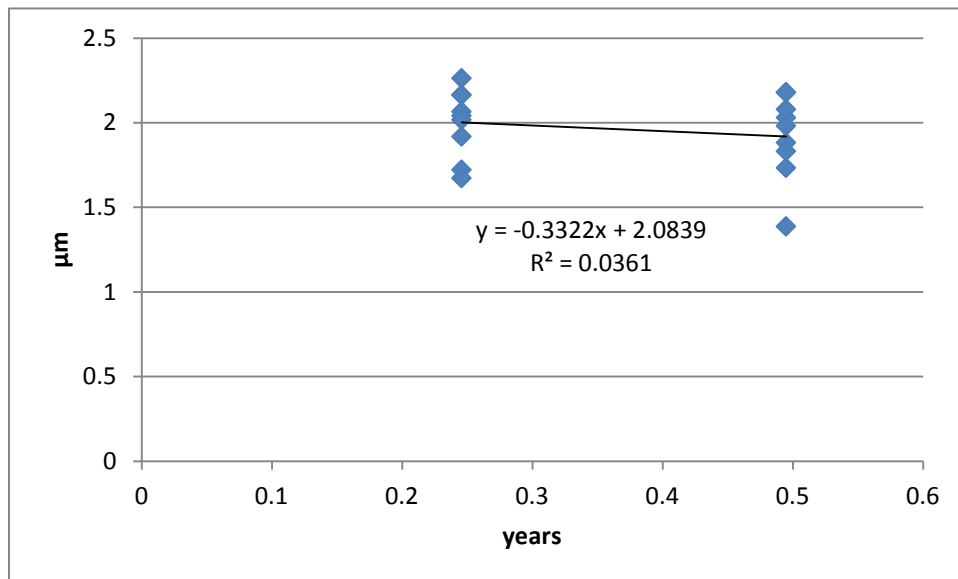
Source: Westerman et al., 1988 for PBB1 brine in salt with 20% H_2O and 90⁰C

Figure 2-4. Corrosion Penetration Depth versus Time - Example 2

2.2.2.3   Factors Effecting the Anoxic Corrosion Rates in Brines

From the data in the cited references, the parameters showing the largest influence on the anoxic corrosion rates of carbon steels in brines are the brine composition and the temperature. Additional parameters considered include alloy composition, sample treatment including welds, salt-brine ratios, test duration, H_2 pressure, gamma radiation, and oxygen contamination of the tests.

Brine Composition and Temperature

Tables 2-4 and 2-5 and Figures 2-1 and 2-2, show that both brine composition and temperature play large roles in the corrosion rates of carbon steels in brines typical of salt repositories. In both Figures 2-1 and 2-2, it can be seen that the corrosion rates increase with temperature, with estimated activation energies of about 13 kcal/mol (53 kJ/mol) for the high-Mg brines and about 6 kcal/mol (26 kJ/mol) for low-Mg brines. The increase in rates with temperature is somewhat greater for high-magnesium brines than for low, as can be seen more clearly by the slopes in Figure 2-5, which shows the data from Figures 2-1 and 2-2 on one plot. However, these slopes are significantly influenced by the few data points at low temperature and are quite uncertain due to the spread in the data. The difference in behavior has been attributed by Kursten el al. (2004) to several effects, the high-Mg brines have higher chloride concentrations, high-Mg brines inhibit the formation of a protective magnetite layer on the metal surface, and high-Mg brines attain lower pH values especially at high temperatures. The effects of brine composition, including pH and the concentrations of Mg, H_2S and $B(OH)_4^-$, are discussed next.
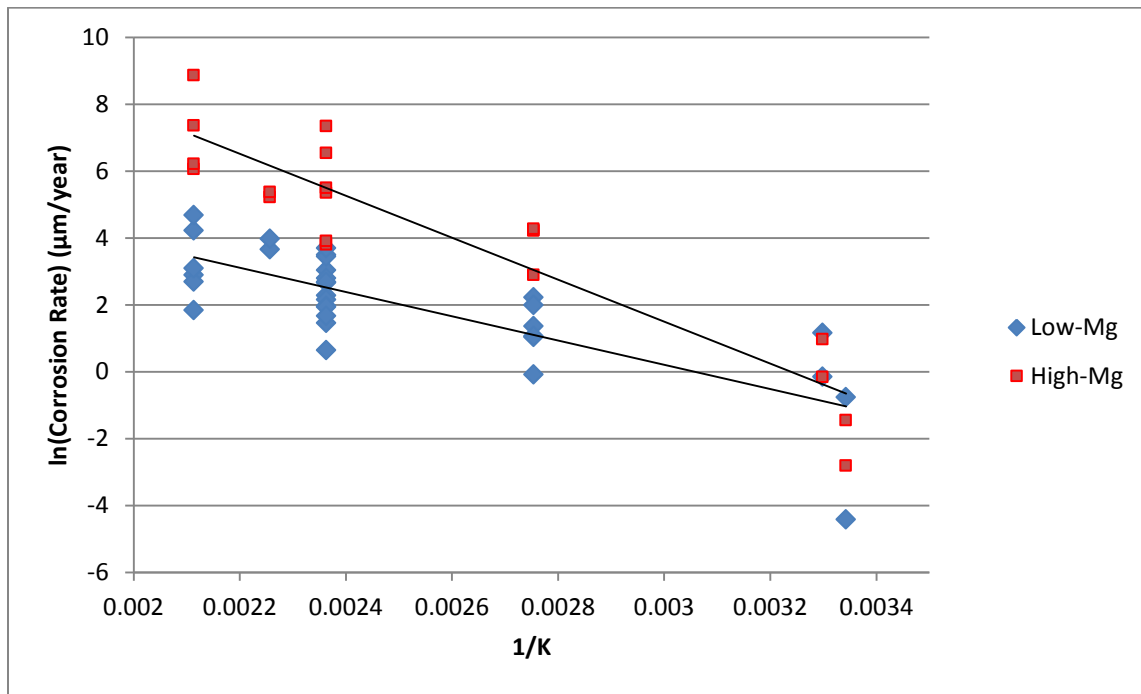
Figure 2-5. Corrosion Data for Carbon Steels in High and Low Magnesium Brines (Summary of Figures 2-1 and 2-2)

Magnesium Concentration

In early corrosion studies of steels, it was assumed that minor differences in the lesser components of brines (e.g., K^+, Mg^{2+}, Ca^{2+}, HCO_3^-, etc.) would probably result in very minor differences in test results and it was inferred that trace components in the brine (i.e. less than ca. 1000 ppm) may cause only second-order changes in waste package interactions compared to changes in brine corrosivity caused by effects of gamma irradiation and oxygen concentration (Molecke, 1983).

Subsequent studies by Westerman and co-workers (Westerman et al., 1986) demonstrated that exposure of carbon steel to halite-saturated brines with high concentration of Mg^{2+} (such as PBB3-type brines with 48,000 ppm Mg^{2+}) results in significantly higher corrosion rates compared to those found in lower magnesium brines, with a concomitant high concentration of Mg found in corrosion products. The same authors investigated the effect of varying Mg^{2+} concentration (1,000, 5,000 and 10,000 ppm Mg^{2+}) in PBB3-like brines on the general corrosion rate of A216 steel (in the as-cast and normalized conditions) through a series of autoclave tests at 150°C with anoxic conditions (Westerman et. al., 1988, p. 6.21). After each test with these relatively low Mg concentrations, the samples were covered with a thin and uniform corrosion product layer with a spinel structure and stoichiometries F_3O_4, $MgFe_2O_4$ or intermediate compositions. However, since corrosion products were characterized with XRD in the study of Westerman and co-workers, it was not possible to determine the exact composition of the spinel phases, and techniques capable of determining the Mg content of the structure (Mg^{2+} is expected to substitute in part for Fe^{2+} in the $Fe^{2+}Fe^{3+}_2O_4$ spinel structure) would be required to determine the specific spinel composition. At the high Mg concentration of PBB3 brine (60,000 mg/L), the corrosion product was identified as amakinite, a complex ferrous magnesium hydroxide, by XRD.

The average corrosion rates of A216 steel vs. Mg^{2+} concentration in halite-saturated PBB3-like brines over 1- and 6-month test durations at 150 °C are shown in Figure 2-6 (Westerman et. al., 1988, Appendixes A and F). Under the test conditions, the increase of corrosion rate with Mg^{2+} concentration is essentially linear. Some diminution of the corrosion rate is observed over time, as seen by the decrease in corrosion rate for the 6-month test compared to the 1-month test. The authors note the correspondence of corrosion rates with the identity of corrosion products. It should be noted that the chloride content of these brines was not reported, and would have changed with the Mg^{2+} concentration; it is not known how much the change in chloride concentration may have contributed to the results.
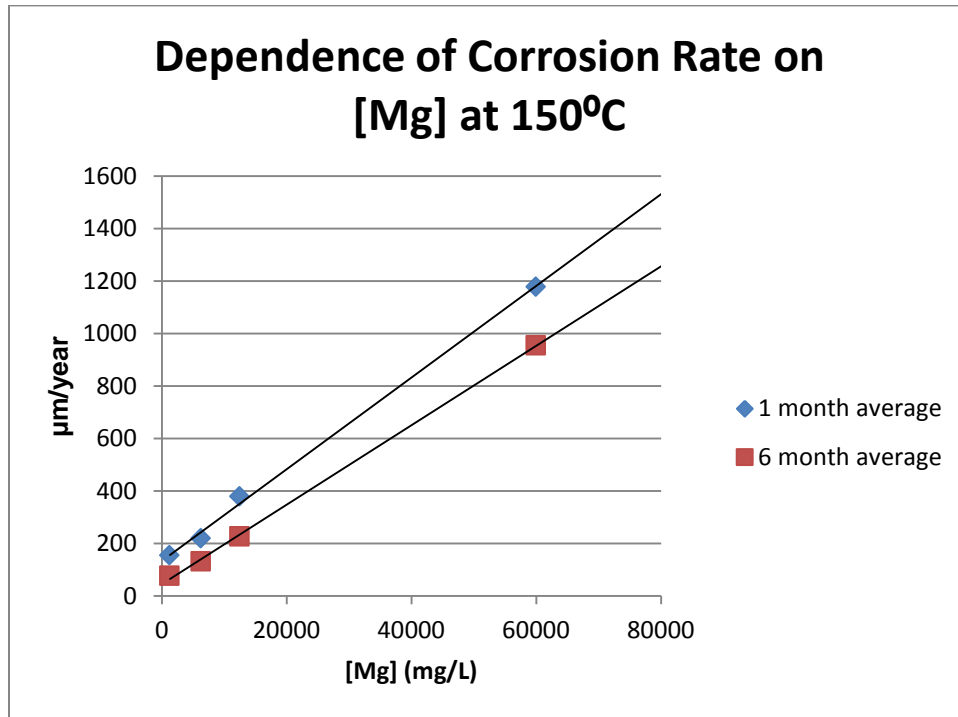
Figure 2-6. Average Corrosion Rates of A216 Steel vs. Mg^{2+} Concentration in Halite-Saturated PBB3-Like Brines Over 1- And 6-Month Test Durations at 150°C (Westerman et. al., 1988).

pH

As discussed in Section 2.1, lowering the pH (increasing the H^+ concentration) can result in the HER becoming a thermodynamically viable cathodic reaction. Since the HER is charge-transfer controlled, higher reaction rates are possible than with the ORR, and as such lower pH values are correlated with higher corrosion rates. In addition, reducing the pH will change the chemical species and thus the anodic reactions which are thermodynamically viable, as discussed in Section 2.2.2.1.

The impact of varying the pH in chloride-rich brine can be seen in the 30°C data of Telander and Westerman (1997) for low-carbon steels A366 and A570 in the low-Mg ERDA-6 brine shown in Table 2-8. The authors note that the increase in corrosion rate seen at the pH value of 10.6, may be due to experimental error such as the introduction of higher concentrations of O_2 in that anoxic test. The corrosion rates in Table 2-8 are consistent with the Eh-pH diagrams by MacDonald et al. (1979) which show the stability field of Fe_3O_4 under anoxic conditions extending down to a pH value of about 8.9 at 25°C and about 3.3 at 250°C. Therefore at 30°C, conditions are likely favorable for a passivating layer of Fe_3O_4 to form at pH values of 8.6 and above.

Table 2-8. Corrosion Rates of Low-Carbon Steels at Various pH values (Telander and Westerman, 1997)

pH	Test Duration (months)	Average Corrosion Rate (µm/year)
2.8	0.19	8000±740
4.8	6	88±17
7.0	6	51±17
8.6	6	2.0±0.5
10.6	6	3.4±1.9

Kursten et al. (2004, Figures 4-8 and 4-9) reported the role of *initial* solution pH on corrosion rates. The experiments were run with TStE 355 samples in brines 1 and 3 at 170°C for up to 1 year. The initial pH was set to the values in Table 2-9, but the pH was not controlled during the experiments. The pH values after termination of the tests were 4.5 to 4.8 for all the Brine 1 tests and 5.4 to 5.7 for all the Brine 3 tests. The authors suggested that these pH values were due to buffering reactions of the brines with the corrosion products. It is not clear how quickly the pH of the tests achieved the buffered values. The corrosion rates seen over the pH range for Brine 1 were not statistically different, but the corrosion rates in Brine 3 at pH values of 1, 2, and 5 were significantly higher than at pH values of 6 and 10. The lower corrosion rates seen at 6 and 10 were explained by the dense corrosion protection layer observed during metallographic examinations of the samples from these tests.

Table 2-9. Corrosion Rates of Low-Carbon Steels at Various Initial pH Values (Kursten et al., 2004)

Initial pH	Brine 1 Corrosion Rate (µm/year)	Brine 3 Corrosion Rate (µm/year)
1		50
2		42
3	207	
4	209	
5	186	46
6		28
7	177	
10		26
Final pH	4.5 – 4.8	5.4 – 5.7

One reaction that causes acidification of high-Mg brines is the hydrolysis of Mg^{2+} (Westerman et al. (1988):

$$Mg^{2+} + H_2O \leftrightarrow Mg(OH)^+ + H^+ \qquad (2\text{-}15)$$

Because of the greater stability constant for $Mg(OH)^+$ with increasing temperature, this reaction will cause a decrease in pH with increasing temperature. Other reactions that may produce acid

in high-Mg brines are those of Mg^{2+} with SO_4^{2-} or $SiO_{2(aq)}$ (Bryan et al., 2011). In addition, the following reaction may also affect the pH during anoxic corrosion of iron in high-Mg brines:

$$1\text{-x } Fe^{2+} + x\ Mg^{2+} + 2\ H_2O \rightarrow (Fe_{1-x}Mg_x)(OH)_2 + 2\ H^+ \qquad (2\text{-}16)$$

Heating of local minerals within the salt could release HCl in the near field environment, which will also reduce the pH. Carnallite ($KMgCl_3 \cdot 6H_2O$) is expected to progressively dehydrate and decompose between 166 and 186 °C under quasi-isothermal and quasi-isobaric conditions (Emons and Fanghaenel, 1989). Bischofite ($MgCl_2 \cdot 6H_2O$) – commonly found in small amounts in halite salts, which is stable at 25 °C, will thermally decompose according to the successive reactions (Sugimoto et al., 2007):

$$MgCl_2 \cdot 6H_2O \rightarrow MgCl_2 \cdot 4H_2O + 2H_2O \quad \text{at 96 °C} \qquad (2\text{-}17)$$

$$MgCl_2 \cdot 4H_2O \rightarrow MgCl_2 \cdot 2H_2O + 2H_2O \quad \text{at 107 °C} \qquad (2\text{-}18)$$

$$MgCl_2 \cdot 2H_2O \rightarrow MgCl_2 \cdot H_2O + H_2O \quad \text{at 153 °C} \qquad (2\text{-}19)$$

$$MgCl_2 \cdot H_2O + H_2O \rightarrow Mg(OH)Cl \cdot nH_2O + HCl + (1\text{-}n)\ H_2O \quad (0 \le n \le 0.3) \quad \text{at 193 °C} \quad (2\text{-}20)$$
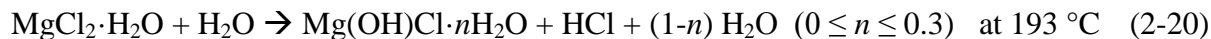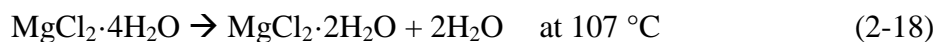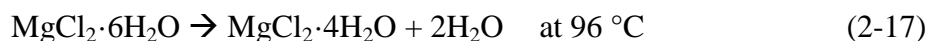
As can be seen from reaction 2-20, temperatures above ca. 193 °C will lead to the production of hydrochloric acid vapors which can increase the corrosivity of the brine. As a matter of fact, several cases of heater failures in Mg-containing salts were reported during the WIPP materials interface interaction tests and attributed to corrosion by hydrochloric acid vapors at high temperature (Molecke, 1986a; Molecke, 1986b). Although small amounts of HCl vapor were believed to be generated, it was suggested that the apparently high concentration of acid found in the brine migration-condensate liquid was caused by the significant concentrating effect of condensing the water and HCl vapors to a liquid (Molecke, 1986b).   The extent of reactions such as 2-20 will be determined by the abundance of the susceptible minerals within the thermal zone around the waste packages. The impact on the pH of solutions in contact with the waste packages will depend on the transport of the brines and gasses including HCl. It is not known whether H_2 gas generated at the waste package surfaces would flush HCl vapors away from the packages and out of the repository, or if the HCl will remain in the immediate vicinity of the packages. In addition, these reactions will only take place during the thermal period and the reverse reactions would be expected to proceed as the repository cools. Given the uncertainties in the extent of these processes, it is likely that assumptions will be made within the repository PAs such that the aforementioned phenomena will not be incorporated. Therefore, obtaining pH dependence of corrosion rates is probably unnecessary for PA purposes.   However, the magnitude of the impact should be assessed such that the effects of pH on the data uncertainty can be incorporated appropriately.

H₂S

It is not clear how much H_2S will be in the repository brines during the time of corrosion of the steels. Kursten et al. (2004) noted that H_2S can be released during heating of the salts from the proposed German repository. They approximated the amounts of sulfides that could be released from 10 cm, 20 cm, and 40 cm thick ring-shaped salt elements around an HLW borehole, as 25 mg/L, 100 mg/L and 200 mg/L of $Na_2S \cdot 9H_2O$ added to their test Q-brine. It was found that sulfides in that range did not significantly influence the general corrosion rates of TStE 355 steel, and did not change the corrosion products detected by XRD. However, Xiong et al. (2012) state that in the presence of iron at elevated temperatures, sulfate is expected to be reduced to sulfide, suggesting that there may be more H_2S formed during corrosion. They note that "*at ambient temperatures, sulfate reduction is usually microbially mediated. However, at elevated temperatures, thermochemical sulfate reduction is frequently observed. For instance, in the southeastern Mississippi salt basin, thermochemical sulfate reduction at temperatures from 100 ℃ to 200 ℃ has been observed in the Smackover Formation (Heydari and Moore, 1989). In addition, dissolved sulfide in the mineralizing brines at 75 ℃ to 200 ℃ responsible for the formation of numerous Mississippi Valley-Type sulfide deposits are also thought to have been produced by thermochemical sulfate reduction (e.g., Anderson and Mcqueen, 1982).*" Machel (2001) reviewed bacterial and thermochemical sulfate reduction in diagenetic settings, and reported that bacterial sulfate reduction was active up to 80℃ and quite fast in geological time, while thermochemical sulfate reduction was operative between 100 and 180℃ and much slower. For example souring of deposits occurred in several tens of thousands to a few million years in the temperature range of 100-140℃. However the reductants in these formations were hydrocarbons instead of iron-based materials, and it is not clear how fast iron or hydrogen gas could bacterially or thermochemically reduce dissolved sulfate at repository-relevant conditions. This is not just an academic question, because at 5 atm H_2S, Telander and Westerman (1997) found that corrosion of low-carbon steels A366 and A570 stopped, apparently due to passivation by FeS. Further literature review and possible tests to investigate sulfate reduction under repository conditions would clarify whether H_2S is produced in sufficient amounts to influence repository performance.

$B(OH)_4^-$

Kursten et al. (2004, p. 80) report corrosion rates in Q-brine at 170℃ with the addition of 0.14 mol/L of the salt impurity $B(OH)_4^-$ to be more than an order of magnitude slower than that of the pure Q-brine. However, the reduction in rates with added borate was not observed at 90℃ and not observed in the NaCl Brine-3 at either temperature. For comparison, the GWB and ERDA-6 brines used by Roselle (2009, Table 2-3) have 0.0473 mol/L and 0.0177 mol/L $B_4O_7^{2-}$, and the Brine A used by Telander and Westerman (1993) was 200 mg/L (0.02 mol/L) boron. The boron content of the German brines and the Westerman et al. brines were not specified.

Microbially Influenced Corrosion

Microbiologically influenced corrosion (MIC) is a process through which bacteria accelerate the corrosion reaction either directly (e.g., attacking the metal) or indirectly (e.g., bacterial metabolites may create a situation where corrosion is enhanced). For MIC to take place, the

environmental conditions must be conducive to bacterial colonization, and species which are capable of impacting the materials of concern must be present. It should be noted that these two requirements are necessary for MIC, _but not sufficient_ – the mere presence of bacteria on a corroding surface does not imply that they have somehow impacted the corrosion reaction. Microbes may influence the corrosion process in a number of ways including the production of acids and sulfides and the consumption of metal ions and hydrogen.   There are three environmental factors necessary for microbial growth: 1) liquid water, 2) an energy source, and 3) nutrients for cell growth. All three could be present in a salt repository. Liquid water in the form of brine will be present during the period of interest (when significant corrosion of the waste package is occurring), the reduction of water or sulfate by steel can provide the energy source for some microbes, and depending on the site, the organic content of the salt and brines may be high. However, at sites where the organic content of the repository is low, microbial growth will be limited.   Westerman et al. (1988) reviewed the literature in the fields of microbiological corrosion, extreme environments microbiology, and waste package design in order to determine whether the conditions in a salt repository are compatible with biological activity. They list four factors that may limit bacterial growth in a repository: 1) temperature, 2) salinity, 3) pressure, and 4) radiation. 1) Temperature - Most bacteria do not grow above temperatures of 70 to 80°C, however some bacterial colonies have been discovered at temperatures up to 300°C when liquid water was present. 2) Salinity - There are a wide range of halophilic bacteria that live and grow well in salty growth media. Westerman et al. (1988) cite Dombrowski (1963) and Reiser and Tasch (1960) who report dormant but viable bacteria in ancient salt deposits. Since the 1960s, there have been a series of additional researchers reporting viable prokaryotes (Bacteria and Archaea) in ancient salt formations, including more recently Holt and Powers (2011). However, Lowenstein et al. (2011) state that extreme longevity of microbes remains controversial.   3) Pressure - Westerman et al. (1988) state "_Hydrostatic and osmotic pressure do not appear to be barriers to bacterial growth in themselves, although the combination of these with high temperature and a radiation field may influence survival and growth rates_." Another factor at lithostatic pressure is the thickness of the brine layer contacting the waste package surface. If this layer is too thin, it will not support the growth of microbial colonies. 4) Radiation - Many common strains of bacteria have shown the ability to adapt to higher radiation levels. The radiation levels at the waste package surface are below the levels needed to completely kill the most radiation-resistant bacteria (Westerman et al., 1988, p. 6.92). Thus individually, the expected repository conditions are within the limits that are tolerated by some microbes; however, it is not clear whether microbes which exist or could evolve in the repository would be able to tolerate all four factors, and also be able to use the water-steel reaction as the energy source. If such microbes exist or evolve, it is not clear how much their growth would influence the corrosion rate. Westerman et al. (1988) note the ability of bacteria to evolve to accommodate changing external conditions, with generation times as short as 20 minutes. They also note the extreme mobility of bacteria in wind and water. They conclude that a salt repository site could potentially support bacteria that would enhance corrosion of carbon steel. However they indicate that further investigation is needed to determine whether the specific combination of conditions in a salt repository will support a corrosive bacterial community as well as the magnitude of the impact of bacterial growth on the corrosion rate.

Alloy Composition and Sample Treatment

A wide variety of carbon steels have been pursued for salt repository and other chloride brine applications, some of which were detailed in Table 2-7. As illustrated earlier in this section, the experimental uncertainty associated with long-term corrosion rate measurements for carbon steel in brine can be considerable. In some cases, as will be discussed below, microstructural changes, such as those brought about by welding, or post-processing heat treatments such as normalization, appear to have some impact on the corrosion rate.

Westerman et al. (1988) performed nearly all their A216 corrosion tests using as-cast, normalized, and welded samples. They note that "*The effect of material condition, i.e., as-cast and normalized, on the corrosion rate was found to be minimal at 90℃, however at 150℃ and 200℃ an effect became apparent, with the normalized material corroding at the higher rate.*" (Westerman et al., 1988, p 6.4) This effect appears to be small however, as the average one-month rates in PBB3 brine at 200℃ were 5.9 mm/year for as-cast and 6.4 mm/years for normalized samples (Westerman et al., 1988, Table 6.1). Under those same conditions, the welded samples showed more variability, but generally lower rates, averaging 3 mm/year. The rate variability was ascribed to the variable fraction of the sample surface area comprised of weld material, ranging from 45 to 100%. The weld material had lower carbon content than the base material, and thus a lower inherent corrosion rate. "*Because the A216 steel parent plate has a great deal more pearlite phase, hence Fe_3C, in its microstructure than the low-carbon weld metal, the parent plate is cathodic to the weld metal, and so enhances corrosion of the weld metal near the weld-metal/parent-plate interface. High corrosion rates are thus associated with approximately equal areas of A216 steel parent plate and weld metal. If either the parent plate or the weld metal is present in very small amounts, the corrosion rate of the specimen approaches the inherent corrosion rate of the dominant material.*" (Westerman et al., 1988, p. 6.4)

Smailos et al. (2004) evaluated TStE355 carbon steel in $MgCl_2$ rich Q-brine and a NaCl-rich brine following a variety of differing thermal processing procedures. Material was evaluated unwelded, welded (both electron beam and tungsten inert gas welded), and welded and aged (600°C for 2 hours). Specimens were exposed for over 500 days at a temperature of 150°C. While the corrosion rates were universally higher in the Q-brine, the corrosion rates from material to material were very similar, with the average values typically within a single standard deviation of one another. As with the studies discussed previously, the uncertainty associated with the measured corrosion rates was substantial. However, based solely on the average values, the corrosion rate of the welded samples was typically slightly higher (0-50% higher in the Q brine, and 20 to 25% higher in the NaCl brine).

Thus, while the composition and underlying microstructure may have an impact on the corrosion process for some combinations of steel and environment, the effect is minor when compared to the experimental uncertainties associated with the corrosion of carbon steel in chloride rich brines.

Brine/Salt Ratios

Most of the tests whose results are reported in Tables 2-4 and 2-5 were performed with the samples immersed in brine. However, the tests of Westerman et al., 1988 in PBB1 brine (reference C in Table 2-5) were performed in dried salt with added PBB1 brine to achieve weight percents of water in the test vessels of 5% or 20%. Comparison of the results at 150°C for this data set for A216 steel (13.3 and 9.8 μm/year) to that from immersed PBB2 brine (14.6 μm/year) shows that there is no statistically significant difference in corrosion rates. Similarly, comparisons of rates in PBB3 brines (Westerman et al., 1988, Appendix B, D and J) with varying brine/salt ratios show no significant differences. At 150°C, the corrosion rates in brine alone were 0.7 to 1.5 mm/year, in a mixture of PBB1 salt and PBB3 they were 0.21 to 1.49 mm/year, in a mixture of surrogate salt and PBB3, they were 0.19 to 1.3 mm/year, in a mixture of surrogate salt with PBB3 brine that had 20 wt% H_2O they were 0.08 to 1.07 mm/year, and in a mixture of surrogate salt with PBB3 brine that had 5 wt% H_2O they were 0.12 to 0.96 mm/year. The lack of significant difference in rates at 150°C is consistent with the hypothesis that since the brine was added to dried salt, the brine was in the intergranular spaces and thus available to be wicked to the sample surfaces. It is not clear that the same would be true in a repository, where H_2O availability at the waste package surface could limit the corrosion rate. Migration of brine toward the hot waste packages is the subject of another test plan and will not be discussed here.

Test Duration (Role of Corrosion Products)

There are some unexplained differences in the effect of test duration on corrosion rates between Kursten et al. (2004) and Westerman et al. (1988).

The corrosion rates reported by Kursten et al. (2004, Tables 4-5 and 4-6) that are reproduced here in Tables 2-4 and 2-5, are the slopes of linear regressions of the depth of attack versus time. Plots of the data show linear response from the first to the last testing times (up to 4 years), but in some cases the rates between start of the experiment to the first data point was somewhat higher as shown by an intercept statistically above zero. This higher initial rate may be due in part to the oxygen present at the start of the experiments (see Oxygen Contamination below). Although the rates in high-Mg brines were between 6 and 25 times faster than those in low-Mg brines, the linear rates suggest that the corrosion products are not protective. The corrosion products observed at 90°C in brine 1 were α-Fe_2O_3 and Fe_3O_4 and in brine 3 were Fe_3O_4 and β-FeOOH, while at 170°C in brine 1 were $(Fe,Mg)(OH)_2$ with no evidence of Fe_3O_4 and in brine 3 were only Fe_3O_4.

Unlike Kursten et al. (2004), Westerman et al. (1988) did not always see a linear depth of attack with time. The tests in salt with the low-Mg brine (PBB1) at 150°C showed a decrease in corrosion rate between the 1 month (8-14 μm/year), 3 month (7-12 μm/year), and 12 month (1-4 μm/year) test periods, with an overall four-fold reduction in rate over the year. The corrosion product was an adherent coating of magnetite (Fe_3O_4). The tests in salt with the high-Mg brine (PBB3) at 150°C showed a smaller decrease in rate, with average corrosion rates from 1 month (620 μm/year), 3 month (670 μm/year), 9 month (420 μm/year), and 12 month (250 μm/year) test periods, and a reduction of about 2.7 between the 3 and 12 month periods. In contrast, a

decrease in rate was not observed for tests in PBB3 brine-only. The authors attributed this difference to the falling away of the corrosion products in the brine-only tests, whereas in the salt/brine tests, the salt held the corrosion products against the metal. The corrosion product both on and below the samples in the PBB3 brine tests was identified by XRD as amakinite, a $(Fe,Mg)(OH)_2$ mineral.
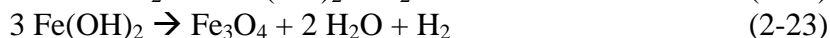
While there is consistency in the linear behavior seen by Kursten et al. (2004) and Westerman et al. (1988) in high-Mg brine-only tests, there is inconsistency in the behavior seen in the low-Mg tests; Westerman et al. saw a decrease in rate but Kursten et al. did not. At this time there is no explanation for this discrepancy.

The corrosion products seen by Kursten et al. (2004) at 170ºC are consistent with that seen by Westerman et al. (1988) at 90 ºC, 150 ºC, and 200 ºC, but at the lower temperatures Kursten et al. also saw the Fe(III) corrosion products α- Fe_2O_3 and β-FeOOH. A possible explanation for this difference, is that these Fe(III) products formed during the early times when the Kursten et al. (2004) experiments were oxic. These Fe(III) corrosion products were not detected at the end of the higher temperature experiments because either they were reduced once the systems became anoxic at those temperatures, or because they were only trace amounts among the higher amounts of reduced corrosion products.

The difference in corrosion rates in the high and low-Mg brines suggests that the Fe_3O_4 formed in the low-Mg brines is somewhat protective, but that the $(Fe,Mg)(OH)_2$ formed in the high-Mg brines offers only limited protection. This hypothesis is supported by several observations by Westerman et al. (1988). The first observation was from short-term electrochemical tests run at 150ºC in 4.5 M brines with varied Mg^{2+}/Na^+ ratios. The anodic potentiodynamic polarization curves showed a passive region in the no-Mg brine, but none in the high-Mg brines. The cathodic polarization curves in high-Mg brines suggest that corrosion in these brines are cathodically rate limited and that the amorphous, gel-like $(Fe,Mg)(OH)_2$ layer in not very effective as a mass-transport barrier. The second observation came from tests that were performed to see if a magnetite film would remain protective upon exposure to high-Mg brine. The specimens were exposed to NaCl brine for 14 days to ensure a substantially uniform magnetite film was formed. After 1 day exposure to 2.25 M $MgCl_2$, the polarization resistance was much lower, with corrosion rates identical to those of specimens not prefilmed with magnetite. The third observation was the effect of microstructure on the corrosion rates. "*The observation that microstructure strongly affects the corrosion rate in the high-Mg^{2+} brine suggests that the rate-determining processes occur at the metal surface itself. This would be the case if the corrosion product that forms is soluble or if the corrosion product is insoluble but is porous and does not provide a good barrier. Therefore, the observed dependence of the corrosion rate on the microstructure further suggests that the amakinite corrosion product is not an effective corrosion barrier. Conversely, the relatively weak effect of the microstructure on the corrosion rate in low-Mg^{2+} brines suggests that the rate-determining processes do not directly involve the metal surface. This would be the case if the corrosion product film formed a barrier between the metal and the corrosive environment and if the properties of the film determined the corrosion rate. It is conceivable that the magnetite layer could act as such a barrier.*" (Westerman et al., 1988, p 6.68)

H$_2$ Pressure

Besides the HERs (reaction 2-7 or 2-8 which result in net reactions 2-21 or 2-22), H$_2$ can be generated by the Schikorr reaction (2-23), where Fe(OH)$_2$ can be further oxidized to form magnetite which is usually more thermodynamically stable (Schikorr, 1933):

$$Fe + 2\,H^+ \rightarrow Fe^{+2} + H_2 \qquad\qquad (2\text{-}21)$$
$$Fe + 2\,H_2O \rightarrow Fe(OH)_2 + H_2 \qquad\qquad (2\text{-}22)$$
$$3\,Fe(OH)_2 \rightarrow Fe_3O_4 + 2\,H_2O + H_2 \qquad\qquad (2\text{-}23)$$
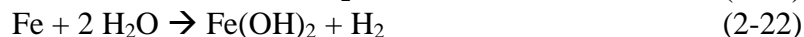
Wall and Enos (2006) calculated the equilibrium H$_2$ fugacities (similar to partial pressures) for reactions 2-22 and 2-23, using thermodynamic data from Chivot (2004), to be ~600 atm and ~500 atm respectively, far above lithostatic pressures of possible salt repositories. (Lithostatic pressure at the 655m repository horizon at WIPP is ~150 atm. The range in repository depths is assumed to be 305 to 1067m in the reference case). Thus, under expected repository conditions, these reactions will not stop due to H$_2$ overpressure, as the host formation will fracture and release the pressure before that could occur.

In most of the anoxic corrosion experiments of carbon steel in brine, the samples and brine are placed in a reaction vessel and sealed. Initial pressures vary, but hydrogen pressure increases with time. However, Westerman et al. (1988) and Telander and Westerman (1993) performed short-term test with various gas compositions and pressures to determine if there was an effect on corrosion rates. Westerman et al. (1988) found that in 1 month tests with PBB3 brine at 150°C the average corrosion rate decreased by a factor of about 5 under 20.7 MPa (3000 psig, 204 atm) H$_2$ and increased by about 60% under 20.7 MPa of Argon compared to experiments with no overpressure. Similarly, Telander and Westerman (1993) found a five-fold reduction in rates under 35 and 70 atm H$_2$ and between 70 and 90% increase in rates under 73 atm N$_2$ compared to 10 atm N$_2$ in 6 month tests at 30°C in brine A. However in 1997, Telander and Westerman reported 127 atm tests which showed less pronounced effects. The rate enhancement between 10 and 127 atm N$_2$ was found to be 60% and the rate depression between 10 atm N$_2$ and 127 atm H$_2$ was less than 30%. They concluded that the effect of N$_2$ pressure would be inconsequential and the effect of H$_2$ pressure on long-term corrosion rate is insignificant.

Gamma Radiation

In the vicinity of the spent-fuel waste container surface, a gamma radiation field will exist and might possibly impact the corrosion behavior of the metallic materials constituting the waste container in the disposal environment. While the exact dose rate will ultimately depend on the container design and the nature of the waste enclosed inside the container, it was considered whether the radiolytic products formed by the effect of gamma radiation on salt brines (e.g., H$_2$O$_2$, ClO$^-$, and ClO$_3^-$) might influence the corrosion process. The oxidizing and reducing reactive radicals and molecular species produced under irradiation can affect the rate and mechanisms of corrosion. While in pure water oxidizing species such as OH•, O$_2$, H$_2$O$_2$, and O$_2^-$ and reducing species including H, e$_{aq}^-$, and H$_2$ will be produced, additional chloride species such as, e.g., Cl$_2^-$, Cl$_2$, or ClO$^-$, can be generated in highly saline solutions exposed to gamma

radiation. In addition, the absorption of gamma radiation in the semi-conducting protective oxide layers of metals can induce photoradiation effects, which can lead to a change in the corrosion rate by facilitating cathodic/anodic reactions at the oxide/electrolyte interface.

Previous irradiation-corrosion tests of A216 steel in surrogate salt and high-Mg PBB3 brine have shown that the anoxic corrosion rates at 150 ^{o}C do not differ significantly from those obtained in non-irradiated autoclave studies utilizing an excess salt, high-Mg (PBB3-containing) environment at the same temperature (Westerman et al., 1988). The irradiation intensity employed in the tests was in the range 11-25 Gy/h. For reference, a gamma dose rate of 10 Gy/h is relevant to HLW thick-walled steel containers, whose corrosion and mechanical allowances give a wall thickness of about 15 cm. The corrosion product formed on the specimens used in that study was identified as amakinite-type by XRD analysis; similar results from XRD analysis were obtained for steel specimens taken from non-irradiated high-Mg environments. Additional irradiation-corrosion tests of A216 steel in surrogate salt and low-Mg PBB1 brine under anoxic conditions at 150 ^{o}C showed similar corrosion rates for both irradiated and non-irradiated samples. The irradiation-corrosion products identified using XRD were also consistent with those obtained from non-irradiated tests in low-Mg (PBB1-containing) environments: the products were identified as Fe_3O_4 (or $MgFe_2O_4$) and siderite ($FeCO_3$) (Westerman et al., 1988). In addition, it was found in these studies that, under the conditions described above, A216 steel was not significantly more susceptible to non-uniform corrosion (e.g., pitting and crevice-corrosion) compared to specimens tested under non-irradiated-environment conditions.

Additional irradiation-corrosion tests were carried out for carbon steel TStE 355 in salt disposal environments in Germany (Kursten et al., 2004). The influence exerted by gamma radiation on TStE 355 was investigated for a radiation field in the range of $1-10^3$ Gy/h, where the upper-limit dose rate of 10^3 Gy/h corresponds to the gamma dose rate on the surface of a thin-walled (thickness of about 5 mm) HLW-canister. The results of the investigations under irradiation showed that gamma dose rates of $1-10^2$ Gy/h did not affect the corrosion rate of the steels. Only at the very high dose rates of 10^3 Gy/h was a strong influence observed on the corrosion behavior of the investigated steel. Specifically, Kursten and coworker concluded that: 1) the imposition of a γ-radiation field (10 Gy/h) did not affect the general corrosion rate in NaCl-rich brine up to 150°C; 2) in the $MgCl_2$-rich brines, a γ-dose rate of $1-10^2$ Gy/h had no influence of the general corrosion rate; 3) at high dose rates of 10^3 Gy/h, the general corrosion rate increased by a factor of about 10.

Because gamma irradiation does not seem to impact significantly the corrosion of thick-walled steel packaging (with gamma dose rates of $1-10^2$ Gy/h at the surface) in both high- and low-Mg-containing environments at temperatures near 150 ^{o}C, the role of irradiation on the corrosion rate will not be reinvestigated in this test plan.

Oxygen Contamination

One factor that, if not adequately controlled, can create systematic or random errors in the data, is the oxygen contamination of the experiments. Westerman et al. (1986) measured the effect of O_2 concentrations at 150°C and 1000 psi in flowing PBB2 brine on as-cast A216 samples and

found rates of 14 μm/year at ~50 ppb O_2 and 25 μm/year at ~1.5 ppm O_2. However, the recirculation rate of 35 mL/hour did not provide enough oxygen in the "oxic" tests to account for the growth rate of corrosion products, so at least some of the 25 μm/year was due to anoxic corrosion. For comparison, the corrosion rate of carbon steel in water in an open system was about 160 μm/year at 60⁰C (Bechtel SAIC Co. LLC [BSC], 2004, Figure 6-12). At higher or lower temperatures the corrosion rate decreased. Thus, significant oxygen contamination can result in artificially high corrosion rates, and it is important to note the experimental setups used in the tests.

In the U.S., Westerman et al. (1986, 1988) and Telander and Westerman (1993, 1997) used both autoclaves and weld sealed containers for the high temperature tests. The autoclave tests were used for static, refreshed and recirculated brines as well as static salt-brine mixtures (Westerman et al., 1988). In the autoclave tests the containers were flushed with argon to preclude oxygen. In the sealed container tests, the container also went through repeated evacuations and backfills with helium before the inlet tube was welded shut. Telander and Westerman (1993) describe the sealed containers to be all-welded except for the pipe-thread joint with the pressure gauge, and the inlet valves. The containers were given a standard leak test capable of detecting a helium leak rate of $1.2 \cdot 10^{-10}$ atm-cc/second. They describe the autoclaves as being less gas tight than the seal-welded containers since the autoclaves have high-pressure gasket seals. Because these vessels were pressurized during the tests, leakage should be from the inside out, and thus oxygen influx should be negligible. Also in the recirculated brine autoclave tests, the brine reservoir was continually sparged with argon, with measured O_2 contents of <50 ppb (Westerman et al., 1988).

Kursten et al., 2004 report the O_2 content of their test brines in the range of 0.6 to 4.9 mg/L but do not describe the experimental procedures. However, additional results reported by Kursten et al. in their Tables 4-5 and 4-6 were from a series of tests performed by Smailos and coworkers between 1992 and 2002. Smailos (1993) summarizes the experimental conditions for the 18-month tests at 150⁰C as follows. The tests were performed in stainless steel pressure vessels with polytetrafluorethylene (PTFE) liners. The initial test conditions were oxidizing with about 0.38 mg O_2/cm^2 of specimen. The O_2 was consumed by reaction with the specimens, and after a few days reducing conditions were established. "*The pressure in the vessels during the tests was 0.4 MPa, which corresponds to the vapor pressure of the brine water at the 150⁰C test temperature. No additional gas pressure by formation of corrosion hydrogen by the reaction of iron with H_2O was measured. This indicates that the hydrogen formed during the test had escaped through the PTFE inserts.*" They calculated the contribution of oxygen to corrosion to be from ~3 to 8% for the 70-day experiments and less for the longer-term experiments.

At lower temperatures, pressure vessels were not always used. Telander and Westerman (1997) performed constant pH tests at 30±5⁰C in glass resin kettles fitted with a plexiglass cover sealed with a neoprene o-ring. The cover had several polyethylene tube fittings for insertion of thermocouples, sparge gas, and sparged acid and base solutions. The sparge gas was > 99.93% N_2. This system was not as leak-tight as the pressure vessels, and some oxygen contamination may have occurred. Roselle (2009) used a mixed-flow gas control system, fit with a set of oxygen traps and an oxygen sensor installed at the gas outlet, for its 26⁰C tests. They did not report any sensor readings, so it is not clear how well the oxygen levels were controlled.

The role of possible O_2 contamination in the above experiments is not clear, but needs to be considered when reviewing the data or designing test set-ups. In particular, the early corrosion rates in the tests reviewed by Kursten et al. (2004) are influenced by the initial oxygen in those tests. For this data, regression analysis using the later time periods was used to obtain the corrosion rates reported by Kursten et al. and plotted in Figures 2-1 and 2-2.

2.2.2.4 Summary Discussion of Data

There exists a significant amount of data for the corrosion of carbon steels in anoxic brines, but there is a large spread in these data as seen in Figures 2-1 through 2-4. As described by Kursten et al. (2004), corrosion is non-uniform general corrosion. They report the maximum penetration depth of this uneven corrosion corresponded to the average depth of attack. The non-uniform nature of the corrosion may explain some of the spread in the data, particularly for small sample sizes.

Differences between data sets by different workers may be due to a number of factors, most likely because different carbon steels were used and the Mg concentrations in the high-Mg brines were not equal. Other effects that may have caused differences include 1) test duration, 2) the experimental pressures, 3) the amounts of minor constituents, 4) the brine/sample area ratios; and 5) the degree of oxygen contamination.

2.2.3   Corrosion Products

As briefly discussed above, the nature of the corrosion products formed under different local environmental conditions in salts strongly affects the corrosion rates. In addition, the corrosion products may control the long-term pH and reduction-oxidation state of the repository system. In particular, Fe(II) containing corrosion products have the potential to maintain radionuclides in their lower valence states, thus rendering them less soluble and reducing radionuclide releases. Therefore, establishing the identity of corrosion products formed in the ranges of brine compositions and temperatures expected in a heat-generating waste disposal system in salt would provide the first step in obtaining the data on these phases necessary to predict their impact on repository performance.

Westerman et al. (1988, p. 6.21) have shown that the corrosion product changed with the Mg^{2+} concentration in Na/K/Ca/Mg-chloride brines at 150 °C. At Mg^{2+} concentrations of 10,000 ppm (12,500 mg/L) or less, the specimens were covered with a thin uniform corrosion product layer, which XRD analysis showed to have a spinel structure, and consisted of Fe_3O_4, $MgFe_2O_4$ or a compound of intermediate stoichiometry. However, the Mg content of the corrosion product was not determined. This identity of this spinel is important to repository performance because Fe_3O_4 has Fe(II) and will help keep the Eh of the system low, while $MgFe_2O_4$ does not. At higher Mg^{2+} concentrations, a clay-like complex Fe/Mg hydroxide was found which was identified as amakinite by XRD. In one year tests in salt and PBB3, the thick corrosion product layer was sectioned and chemically analyzed (Westerman et al., 1988, p. 6.32). Across the sections the Fe ranged from 22 to 28 wt% moving from the outside to the sample surface, but the Mg remained constant at about 6 wt%. They speculate that the decrease in Fe from the inner to outer layers

may be due to a decreasing Fe concentration in the liquid phase rather than the solid reaction product. The increasing Na and Cl from the inner to outer layers may be due to brine in the pores of the corrosion product. Assuming an amakinite-only corrosion product with 25 wt% Fe and 6 wt% Mg, the chemical formula would be $Fe_{0.64}Mg_{0.36}(OH)_2$, which is somewhat similar to that reported for amakinite in the mindat.org website $((Fe_{0.73}Mg_{0.22}Mn_{0.05})(OH)_2)$. Similar attempts by Telander and Westerman (1993, 1997) at identifying the $(Fe,Mg)(OH)_2$ phase formed in their high-Mg brine tests at 30°C have been unsuccessful. The XRD (Figure 2-11) gave a distinct pattern that does not match amakinite or any other related compound. The sharp diffraction peaks displayed in this figure demonstrate that the corrosion product analyzed exhibit crystalline characteristics (amorphous corrosion products would result in broad diffraction peaks with a lack of distinctive features). Chemical analysis of filtered, washed corrosion product showed weight percents of ~38 for Fe, ~7 for Mg, ~0.18 for Mn, for a chemical formula of $(Fe_{0.700}Mg_{0.297}Mn_{0.003})(OH)_2$.

Roselle (2010) examined the 26°C samples immersed in E-GWB and E-ERDA-6 brines and identified only two phases by scanning electron microscopy (SEM) and energy dispersive spectroscopy (EDS), "Iron chloride 1" and "Iron chloride 2". Iron chloride 1 was found on all the immersed samples and was identified by EDS as an iron/magnesium-chlori-hydroxide, whose O peak was greater than the Cl peak. This phase exhibits an angular or blocky habit. Iron chloride 2 was found on only a few samples, including the samples in E-ERDA-6 brine. It is often comingled with the iron chloride 1 phase and is identified as an iron-chlori-hydroxide with little or no magnesium and a Cl peak larger than the O peak. It is found as aggregates or rosettes of plate-like crystals.

ID: 1013928 Container #25 Corrosion Product (wet)

File: 101392B.MDI   Scan: 5-75/.02/1/#3501, Anode: CU   Zero=0.0
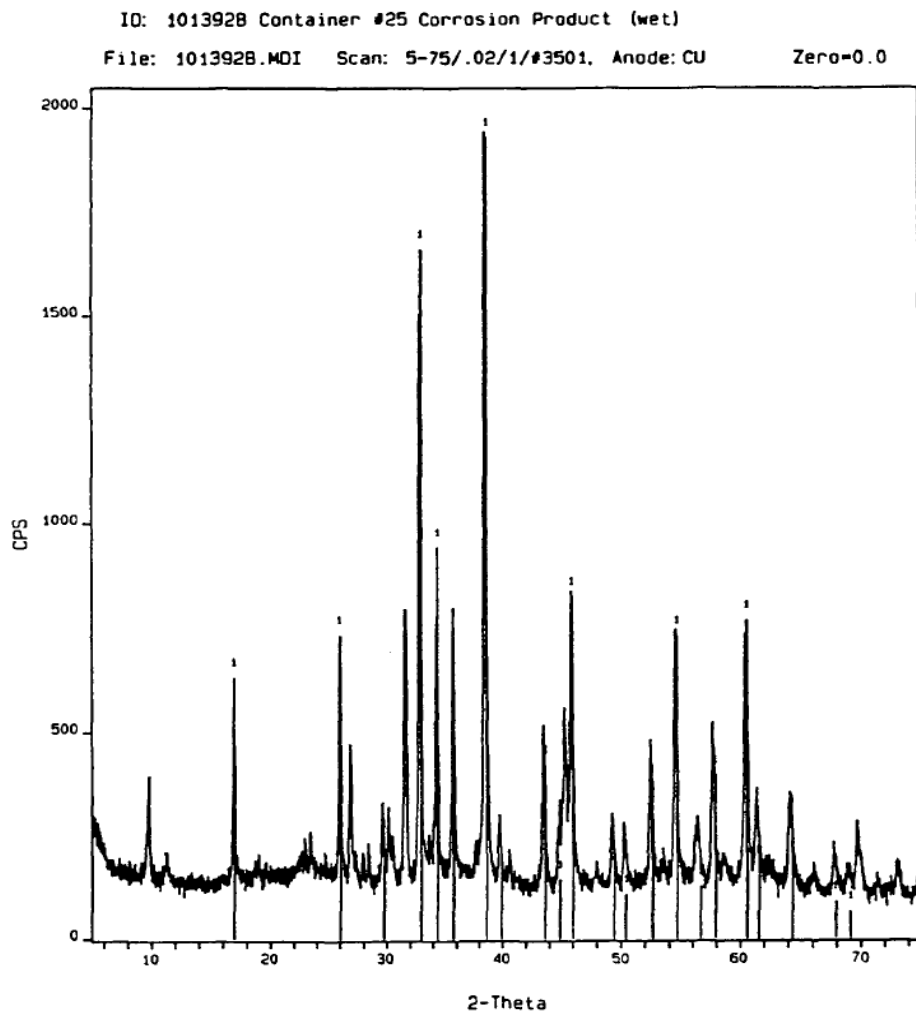
Notes: Telander and Westerman (1997), Figure 6-4. The vertical lines (labeled "1") correspond to the principal-12-month corrosion-product diffraction peaks; they are superimposed on the raw data obtained from the 24-month corrosion product. More than one compound may be present in each lot of corrosion product.

Figure 2-7. XRD Results Obtained from the Unidentified 12- and 24-month-Test Corrosion Products, Anoxic Brine Tests.

2.2.4   Data Gaps

Because there is inconsistency in the temporal behavior of carbon steel corrosion rates in anoxic brines, further work is warranted. In particular it is not clear why the Kursten et al. (2004) data showed constant corrosion rates while Westerman et al. (1988) saw decreasing rates in low-Mg brines. Also, the decrease in rates seen in salt + Mg-rich brine mixtures by Westerman et al. (1988) should be confirmed for time periods longer than 1 year.

It is unknown whether microbes will significantly influence the corrosion rates within a salt repository. However, the likelihood of significant influence is site-specific and does not lend itself to investigation prior to site selection. Therefore microbiologically influenced corrosion will not be investigated under this test plan.

A systematic investigation of the thermochemical reduction of sulfate by steels or hydrogen will not be undertaken; however tests for H_2S or FeS formation should be conducted when the test vessels are opened.

The identity of the corrosion products over the full range of repository-relevant temperatures and Mg concentrations has not been determined. Particularly needed are: 1) the identity of the $(Fe_{1-x}Mg_x)(OH)_2$ corrosion product produced in high-Mg brines at 30⁰C, 2) confirmation of amakinite as the $(Fe_{1-x}Mg_x)(OH)_2$ corrosion product in high-Mg brines at high temperatures, 3) determination of the conditions where the spinels F_3O_4, or $MgFe_2O_4$ form instead of $(Fe_{1-x}Mg_x)(OH)_2$, and 4) the Mg content of any spinels that form. Based on experiments to date, the spinels only form at low Mg concentrations and high temperatures.

A test matrix of three temperatures 30, 90, and 150⁰C and the two brines, one high in Mg, and one low in Mg, would span the conditions needed for the long-term tests and for items 1 and 2 above. (See Section 3.2.1 for the selection of Brine A and PBB2 for the high and low Mg brines respectively.) For items 3 and 4, Westerman et al. (1988) have shown that at 150⁰C a spinel forms at Mg concentrations of ≤12,500 mg/L and amakinite forms at 60,000 mg/L. The proposed tests will determine what corrosion products form at 35,000 mg/L (Brine A), and what corrosion products form at lower temperatures.

2.3   Corrosion of Stainless Steel in Anoxic, Chloride Rich Brines

2.3.1   Background

As discussed above, the reference waste package consists of a thin-walled (10 to 20 mm) stainless steel canister surrounded by thick carbon steel overpack, both sealed with welded closures. A variety of austenitic stainless steels have been proposed (based upon their use in other similar applications), including 304 and 316. The purpose of the overpack is to resist package breach due to crushing or buckling, and for this document is assumed to have a thickness of 7.5 cm. When the overpack (carbon steel) is first breached, the carbon steel will provide cathodic protection for the exposed stainless (acting as a sacrificial anode) until enough

carbon steel has been removed from the area around the exposed stainless steel that it is no longer able to exert electrochemical control over the exposed stainless. At that point, the overpack can be considered to have been effectively removed due to general corrosion, and corrosion of the stainless steel inner canister may take place. It should be noted that the environment which ultimately comes into contact with the inner container will be controlled not only by the brine from the surrounding salt, but by the voluminous corrosion products remaining from the carbon steel as well. The corrosion product layer remaining from the overpack will be considerably thicker than the initial 7.5 cm of steel. As a result, in addition to the normal brine constituents, the environment at the stainless steel surface once the overpack is breached will contain high concentrations of iron ions (likely ferrous, due to the anoxic nature of the brine) which will modify the pH (due to metal ion hydrolysis) and further increase the susceptibility of stainless steels to localized corrosion. In addition, the brine will be anoxic, as any dissolved oxygen would have been long consumed via the ORR during the corrosion of the carbon steel overpack.

Unlike carbon steel, stainless steels are fairly resistant to general corrosion in a variety of environments, but can be susceptible to localized corrosion (i.e., crevice corrosion or pitting), particularly in chloride-rich environments. The corrosion resistance of stainless steels is due to the formation of a protective chromium oxide layer on the metal surface. This passive film, while providing outstanding corrosion resistance in many environments, can be broken down locally in the presence of halide ions, such as chloride. This leads to localized corrosion, such as pitting or crevice corrosion. In such cases, while the general corrosion rate may be low, the corrosion rate at specific sites (e.g., pits) can be extremely large, leading to perforation of the material long before general corrosion might compromise the structure. While high concentrations of chloride will also enhance the general corrosion rate, localized corrosion is the dominant failure mode for stainless steels in chloride brines.

In order to assess the performance of the stainless steel inner container in a salt repository, the literature was reviewed, focusing on the corrosion behavior of austenitic stainless steels in anoxic brine.

2.3.2   Corrosion Behavior of Stainless Steel in a Salt Repository

Stainless steels are very resistant to general corrosion in a variety of environments, including high salinity brines, particularly when compared to the carbon steels discussed in the sections above. However, they can be very susceptible to localized corrosion, such as pitting. Since the localized rate of attack can vary considerably from point to point on a stainless steel surface, the overall corrosion behavior has been considered to be less predictable than a corrosion allowance material such as carbon steel. As a result, it has not been considered as a material of construction for salt repositories such as that proposed by Germany (Kursten, 2004). Since it was not considered a viable containment vessel, there is considerably less work in the literature from which long-term corrosion rates, general or localized, can be drawn. In this section, the data that is available will be reviewed.

Several stainless steels (304L and 309S) were screened for use in the German repository concept in $MgCl_2$ rich brines (Q-Brine with 26.8 wt% MgCl2 and a 45 wt% $MgCl_2$ brine at 180°C for 504 days). Both materials exhibited significant intergranular attack (greater than 2 mm into sample), pitting corrosion (120 um deep on 304 and 30 micron deep on 309S), and stress corrosion cracking. General corrosion rates were lower, 1.2±0.7μm/yr for 304L and 1.0±0.6μm/yr for 309S for unwelded material, and slightly higher for welded material (Smailos, 1999; Kursten, 2004). As the goal of that work was to establish a material which exhibited predictable corrosion performance, they were eliminated from consideration, and no further studies were performed.

In addition to salt repositories, other areas where the behavior of stainless steel in anoxic brines has been pursued include geothermal wells and desalination plants. Cramer and Carter (Cramer and Carter, 1980; Carter and McCawley, 1982) explored the corrosion performance of 430SS, 316L SS, and E-Brite 26-1 (a 26Cr-1Mo ferritic stainless steel) in the Salton Sea geothermal area. Materials were evaluated in the lab as well as in-situ at the actual well head. There was considerable disagreement between the corrosion rates in the lab and for coupons placed in the actual well (the latter being much higher) and for that reason, the results from the laboratory will be discussed here, as it is not clear if the inconsistencies with the field are the result of periodic chemical fluctuations, or some other factor. The composition of the brine used in the laboratory studies is given in Table 2-10.

Table 2-10. Composition of Salton Sea Brine (Cramer and Carter, 1980)

Salton Sea Brine	ppm
Na	53000
Ca	28800
K	16500
Fe	2000
Mn	1370
Zn	500
Sr	440
Si	190
B	390
Ba	250
Li	210
Mg	10
Cl	155000
S	30

In deaerated brine, the general corrosion rates for all 3 stainless steels were very low, until oxygen was introduced into the system. (Table 2-11) This is in sharp contrast to the carbon steels, where dissolution rates in excess of 7 mm/year were observed for some of the materials. In addition to the general corrosion rate, the tendency and rate of localized corrosion was also monitored. Under deaerated conditions, all three of the materials evaluated were resistant to

localized attack, with no observation of pitting on any of the materials (see Table 2-12), though 316L was found to be susceptible to crevice corrosion. Upon the introduction of oxygen to the system, the rate of localized attack increased dramatically, as shown in the table. Thus, while the likely mechanism through which the stainless steels will degrade in concentrated brine is localized corrosion, such as pitting, the rate of such attack will likely be dramatically reduced under anoxic conditions. It should also be noted that while the brines evaluated in the Cramer and Carter work contained a high concentration of chloride, the metal ion content (e.g., ferrous ion content) was low. This will differ from the environment likely to exist at the stainless steel surface once the overpack has been breached. The elevated metal ion content will be considerably higher, and the tendency to initiate and support localized attack also increased. In practical terms, the localized nature of the attack means that the rate and nature of failure of the stainless steel will be inherently unpredictable. While some areas will fail completely due to perforation by localized attack, nearby regions might be completely unimpacted.

Table 2-11. General Corrosion Rates of Stainless Steels in Salton Sea Brine (Cramer and Carter, 1980)

	Deaerated Salton Sea, 232°C, 15 days (μm/year)	Aerated (100 ppm O$_2$) (μm/year)
430SS	0	8760
316L	0	4010
E-Brite 26-1	3	530

Table 2-12. Pitting Rates of Stainless Steels in Salton Sea Brine (Cramer and Carter, 1980)

	Deaerated Salton Sea, 232°C, 15 days (μm/year) (maximum/average)	Aerated (100 ppm O$_2$) (μm/year) (maximum/average)
430SS	0/0	Detected
316L	0/0	5100/3300
E-Brite 26-1	0/0	24300/21000

Another test program which looked at the long-term corrosion performance of stainless steel in brine was the Materials Interface Interactions Test (MIIT) performed for the Waste Isolation Pilot Plant (WIPP) completed in 1991 (Molecke and Wicks, 1992). In this test, samples of a wide variety of materials were placed in wells filled with brine and located within WIPP (bedded salt deposits in the Salado Formation near Carlsbad, NM). Samples were emplaced for a total of 5 years and held at a temperature of 90°C, with representative coupons being periodically removed and evaluated over the course of the experiment. The brine used to fill each sample well was WIPP Brine A (1.83M Na$^+$, 1.44M Mg^{2+}, 0.77M K$^+$, 20 mM Ca^{2+}, 3 mM Li$^+$, 0.2 mM Rb$^+$, 5.35M Cl$^-$, 40 mM SO$_4^-$, 20 mM B (as BO$_3^{2-}$). This brine equilibrated with the host salt, resulting in the precipitation of gypsum, carnallite (KMgCl$_3$·6H$_2$O), bischofite (MgCl$_2$·6H$_2$O)

and other minor constituents. As a result, for the majority of the test period, most of the samples were encased in mostly solid, damp precipitated salts (Molecke and Wicks, 1992). As a result of the limited quantity of brine which was present within the salt, and its availability to the metal surface, it is reasonable to assume that the dissolved oxygen concentration would be low once the system had equilibrated due to cathodic consumption of the dissolved oxygen from the brine.

Among the materials evaluated in the MIIT were 304L (both welded and unwelded), 309, and 316 stainless steel. All of the stainless steels exhibited a weight loss due to corrosion which increased over time. All exhibited no signs of general corrosion, but were susceptible to localized attack (i.e., pitting and crevice corrosion). Furthermore, the 304L material was found to be highly susceptible to stress corrosion cracking, with numerous transgranular cracks observed emanating from high stress regions of each coupon (e.g., the sheared/deformed regions from sample cutting and preparation). (Sorensen and Molecke, 1992)

2.3.3   Corrosion Products

Little information was found in the literature detailing the nature of the corrosion products for stainless steel in brine. While the constituents will clearly be oxides and hydroxides of the alloying elements within the materials (i.e., Fe, Ni, and Cr), the specific species and relative proportions have not been well documented in the literature.

2.3.4   Data Gaps

There are a number of clear data gaps for the corrosion of stainless steels in a salt repository environment which need to be addressed:

1. The environment at the surface of the stainless steel, while it will be a function of the local brine composition, will also include significant contributions from the carbon steel corrosion products which will separate the bulk salt from the stainless steel. It is likely that significant quantities of ferrous, and potentially ferric, ions will be present, which will tend to acidify the brine and render it more corrosive. As such, in order to evaluate the performance of stainless steels in a salt repository environment, the solution chemistry at the stainless steel surface must be assessed.
2. While literature data exists to demonstrate the corrosion performance of many stainless steels in a concentrated chloride brine, no such work was identified where the impact of the corrosion products from the carbon steel were taken into account. As a result, the general and localized corrosion performance, as well as the susceptibility of the various alloys of interest to stress corrosion cracking in a relevant iron-rich brine should be evaluated.
3. Little documentation is available in the literature detailing the specific corrosion products formed by stainless steels in a salt repository. As with the carbon steel, the nature of the corrosion products on stainless steels must also be determined so that their impact on the performance of the repository can be assessed.

3.   EXPERIMENTAL WORK ASSESSING CORROSION OF STEELS IN BRINES

3.1   Materials

Early HLW canister corrosion studies carried out within the WIPP Project used a variety of carbon steels, such as Corten A steel (a low-C steel), Type 1018 mild steel, ASTM 216-77 grade WCA, ASTM A-106 or ASTM A-36 (Braithwaite and Molecke, 1980; Molecke et al., 1983; Molecke, 1984). Other WIPP studies used test specimens made of ASTM A366 (standard specification for cold-rolled sheet; representative of steel waste drums) and ASTM A570 low-carbons steels (standard specification for hot-rolled carbon steel sheet and strip; representative of steel waste boxes and other steel waste materials) (see Telander and Westerman, 1997). Other steels such as the ASTM A36 steel (with 0.25% C maximum and 0.8 to 1.2% Mn) and the ASTM A569 steel (with 0.15% C and 0.60% Mn maximum) were also discussed as possible representative highly-alloyed materials used in the waste boxes. The compositions of some of steels used in tests are presented in Table 2-7.

In the Salt Repository Project, the ASTM A216 Casting Specifications Grade WCA material was considered to be the reference waste package overpack material (cf. composition in Table 3-1). It should be noted that the ASTM specification indicates this material to be supplied in the annealed, normalized, or normalized and tempered condition, although as-cast material was emphasized in SRP tests (Westerman et al., 1986). However, there is no evidence that that the improvement in mechanical properties brought about by heat treatment would be required in the final overpack design.

Ideally, the materials tested would be those actually specified for use in a future repository. In the absence of waste package design specifications, it is recommended that stainless steel type 304L and 316L be tested as possible candidates for the canister, and carbon steel ASTM A216 WCA or A516 grade 70, be tested as possible candidates for the corrosion allowance overpack. For the canister, stainless steel type 304L is recommended for testing because it is a widely used material and is currently being used for high level waste glass pour canisters and used nuclear fuel dry storage canisters. For the YMP program it was planned to be used for the canister to contain the N-reactor fuel (BSC, 2004). Stainless steel type 316 was specified for the inner vessel for the YMP waste package and it has been used for dry storage near the ocean because of its superior corrosion resistance in a salty environment. However it is more expensive than type 304, and superior performance of the canister is not needed in a salt repository, as the overpack provides the structural protection of the waste during the 300 year waste retrieval period. For the overpack, carbon steel ASTM A216 WCA is recommended for testing because it has already been extensively studied as a corrosion allowance material in salt. Carbon steel ASTM A516 grade 70 should also be considered because it was specified as a basket material for the YMP waste packages (BSC, 2004) and will likely be contained within the waste packages. The compositions of these steels are given in Table 3-1.

Table 3-1. Steel Compositions (wt%)

	A216 WCA[a] J02502	A516 grade 70[b] K02700	304L[c] S30403	316L[c] S31603
C	≤0.25	≤0.28	≤0.03	≤0.03
Si	≤0.60	0.15-0.45	≤0.75	≤0.75
P	≤0.04	≤0.035	≤0.045	≤0.045
S	≤0.045	≤0.035	≤0.03	≤0.03
Cr	≤0.50		18-20	16-18
Mn	≤0.70	0.85-1.2	≤2.0	≤2.0
Ni	≤0.50		8-12	10-14
Cu	≤0.30			
Mo	≤0.20			2-3
V	≤0.03			
Fe	Balance	Balance	Balance	Balance

[a] ASTM A216/A216M-08 Standard Specification for Steel Castings, Carbon, Suitable for Fusion Welding, for High-Temperature Service.

[b] ASTM A516/A516M-06 Standard Specification for Pressure Vessel Plates, Carbon Steel, for Moderate and Lower Temperature Service.

[c] ASTM A240/A240M-06 Standard Specification for Chromium and Chromium-Nickel Stainless Steel Plate, Sheet, and Strip for Pressure Vessels and for General Applications.

3.2   Brines and Salts

3.2.1   Brines

A variety of brine compositions has been proposed with particular relevance to high-level waste package materials testing programs, in an effort to be either generic or site-specific or expedient in laboratory testing. Previous studies have discussed in great detail the characteristics of the many different brine compositions proposed or used for corrosion testing of waste package barriers, waste form leachability or backfill and other tests (for details, see e.g. Molecke, 1983). Some of the most representative brines – either analyzed at deposits or used in laboratory tests - and their compositions (major components only) are given in Tables 2-1, 2-2, and 2-6. The brines listed in Tables 2-2 and 2-6 can be classified into two types; 1) high-Na-Mg-K-Cl brines and 2) high-NaCl brines.

While most of the brines listed in Table 2-6 were originally defined as site-specific brines, a few brines have become generic test brines through widespread laboratory usage. This is the case in particular for the so-called Brine A, which was originally defined as a WIPP site-specific brine but gained status of standard brine owing to the early definition and the large amount of experimental work and published results using this brine. Brine A, characterized by its high Na-Mg-K-Cl content, was defined with the intend to represent brines that have interacted with potassium and magnesium minerals and could potentially intrude into a waste facility in bedded salt by percolation through an overlaying zone containing potash. Brine A is based on the early

analyses of several brine seeps from the Salado region in southeastern New Mexico overlaying the WIPP and its vicinity. Brine A's Mg concentration of 35,000 mg/L bounds the weeps and Inclusion group II concentrations in Table 2-2, but does not bound the Inclusion Group I Mg concentration. However, there are far fewer Group I brines than Group II brines, so Brine A is a more representative high-Mg end member brine for the fluids migrating toward the waste package. The German Quinare Brine Q or Brines 1 and 2 have much higher K^+ and Mg^{2+} concentrations than the brines seen in the U.S. as a result of the significant quantities of carnallite ($KMgCl_3 \cdot 6H_2O$) found in close proximity to halite at the Asse and Gorleben rock salt sites that have been evaluated in Germany for a radioactive waste experimental facility or potential waste repository (Molecke, 1983). While the Brines 1 and 2 or the Quinare Brine Q used in the German testing program could be potentially better than Brine A for over-tests of the long-term corrosion resistance of candidate waste package barrier materials, the composition of Brine A is more representative of end-member brines of the bedded salt formations found of the U.S. Therefore, it is recommended to use Brine A to study the influence of Mg^{2+} concentration in the corrosion tests envisioned in this test plan.

The high-NaCl brines resulting from intrusion of brine from outside the repository horizon have less variation than the high-Na-Mg-K-Cl, as seen in Table 2-6. Any of these low-Mg brines except E-ERDA-6 are suitable as end-members for testing, however PBB2 is chosen because it is less likely to have problems with precipitation of brine constituents during the experiments.

Table 3-2. Brines for Experiments (mg/L, ±3%)

	Brine	Na^+	Mg^{2+}	K^+	Ca^{2+}	SO_4^{2-}	Cl^-	BO_3^{-3}	HCO_3^-
A	Brine A	42,000	35,000	30,000	600	3,500	190,000	1,200	700
B	PBB2	123,000	122	39	1,110	1,910	191,000	-	23

A   Molecke, 1983, Table 2
B   Westerman et al., 1988, Table 4.3

3.2.2   Salts

In order to obtain representative long-term corrosion rates, it is important that the corrosion products are held to the sample surface much like the mined salt backfill will hold the corrosion products against the waste package surface. Ideally, crushed salt mined from the repository horizon would be used in the tests to serve this purpose. The generic salt repository reference case assumes that the repository horizon is located in a relatively pure halite stratum that is at least 12 meters thick, with only very thin interbeds and seams of impurities less than 0.25 meters thick (Sevougian et al., 2012). It is expected that the corrosion rates will be relatively insensitive to the salt composition as long as the salt does not contain significant quantities of minerals that could change the Mg concentration of the contacting brine. Therefore pure NaCl is chosen.

3.3   Tasks

3.3.1   Brine Formulation and Analysis

3.3.1.1   Brine Formulation

The brines will be prepared to meet the compositions in Table 3-2 to an accuracy of ±3%, following the example of the WIPP Standard Procedure SP 20-4 (Xiong, 2008). Table 3-3 provides the calculated recipes rounded to 3 significant figures. When the amount of NaCl was calculated based on a sodium balance, it was slightly different than that based on a chloride balance. An average of the two is reported, along with the percent difference between the two. The percent difference was within the assigned accuracy of ±3%. The charge balance error, as defined in SP 20-4, is -0.17% for Brine A and is -0.11% for PBB2.   The room temperature pH for Brine A is reported as 6.5 (Molecke, 1983). While no pH was reported for PBB2, PBB1, which is very similar, had a pH of 7.055. For comparison, WIPP Brine B has a pH value of 6.5. These reported pH values are likely "as measured" and not corrected for effects of the high ionic strengths of the solutions, so should be used with caution. However, if the resulting brines have pH values more than a pH unit different from these, hydrochloric acid or sodium hydroxide may be used to adjust the pH.

Table 3-3. Brine Recipes

	g/L solution	
Component	Brine A	PBB2
NaCl	99.8	311
$MgCl_2 \cdot 6H_2O$	293	1.02
KCl	57.2	0.0744
$CaCl_2 \cdot 2H_2O$	2.20	4.07
Na_2SO_4	5.17	2.82
$Na_2B_4O_7 \cdot 10H_2O$	1.95	0
$NaHCO_3$	0.872	0.0287
H_2O *	740	881
% difference in Na and Cl needed	2.8	-0.22

*assuming a brine density of 1.2.

3.3.1.2   Brine pH and Composition Monitoring

As discussed in Section 2.2.2.3, when pH values were held constant during the carbon steel experiments, the corrosion rate was quite dependent on pH (Telander and Westerman, 1997). However, initial pH did not have a profound influence on the long-term corrosion rates of carbon steel in the German tests because the system controlled the pH to a range of 4.5 to 4.8 in very high-Mg brines and to a range of 5.4 to 5.7 for high-NaCl brines (Kursten et al., 2004). Because

the production of corrosion products may acidify the test solution (see Reaction 2-16), these pH ranges may depend on the extent of corrosion and the brine volume to coupon surface area ratio, which was 2 ml/cm^2 in these experiments. While measuring the solution pH would be crucial to developing a mechanistic model for carbon steel, it is not required for developing an empirical model. However, since the corroding carbon steel overpack will provide the environment for the corrosion of the stainless steel canister, the pH generated by the corroding carbon steel is an important parameter to measure.

The pH values of the test brines should be measured upon each test vessel opening. Thus, in the salt/brine mixture tests, the design setup must include provisions for collection of enough brine for pH measurement. This may be accomplished by the use of a small brine reservoir that is in good communication with the salt/brine mixture. In brines, measurement of an accurate pH using commercially available combination glass electrodes is difficult due to differences in the liquid junction potentials in the test solution versus standard solutions. In addition, it is often the pcH, the negative log of the hydrogen ion concentration, not the pH, the negative log of the hydrogen ion activity, which is desired. These difficulties may be overcome by calibration of the pH electrode and Gran titrations as described by Rai et al. (1995). Such calibration and titrations have been done for WIPP-relevant brines as reported by Roselle (2012). For brines with low Na_2SO_4 concentrations, including NaCl-dominated and high-Mg brines, the resulting correction factor A is a function of I_M, the molar ionic strength of the solution:

$$A (\pm 0.47) = 0.186\ I_M - 0.105$$

This correction factor is applicable for room temperature. The pH of all test solutions should be measured at room temperature, and if possible, at the test temperature as well. For experiments up to 90⁰C, a procedure similar to that detailed by van Middlesworth and Wood (1999) should be used. Specifically, each buffer solution should have the same ionic strength as the test solution, and the pH electrode should be calibrated at the test temperature. At temperatures above 90 ^{o}C, however, glass electrodes cannot be used and high pressure equipment is required, such as a high temperature potentiometric system. If such a system is available, pH values at high temperature should be obtained.

In addition to pH, it is desired to obtain the dissolved element concentrations within the test solutions, including Fe^{2+}. Ideally, the test vessels would permit sampling of solutions at the test temperatures and pressures as described in *Test Plan for Determining Thermodynamic Properties of Brines, Minerals and Corrosion Products for High Level Radioactive Waste Disposal in Salt* by Xiong et al., 2012. Brine samples would be withdrawn, immediately filtered and acidified with trace metal grade concentrated HCl, and diluted for chemical analysis.

3.3.2   Metal Sample Preparation for Corrosion Tests

In order to achieve a high degree of accuracy while minimizing experimental uncertainty in weight loss testing, it is imperative that the surface finish, dimensions, and surface cleanliness of the test coupons prior to the initiation of the test program be tightly controlled, and uniform.

Procedures for proper handling of coupons are described in ASTM G1, and are summarized below.

Surface finish: To the extent possible, the surface finish of all exposed surfaces on the test coupon should be uniform, and nominally identical in terms of surface roughness to that specified for the application being simulated. Surface marking to maintain sample identification should not introduce any foreign material to the test specimen (e.g., a diamond or carbide scribe would be appropriate, but a tool steel punch would not) and be compatible with the extent of corrosion anticipated. (i.e., if significant attack is anticipated, a scribed mark will be rapidly lost due to corrosion – an alternative method such as edge notching would be preferable).

Surface cleaning: Prior to being placed into the test solution, the surface of each coupon should be cleaned of organic contamination and debris such as polishing fines. This can be accomplished with ultrasonic treatment in an appropriate solvent or detergent solution. However, care must be taken when handling materials which are very susceptible to attack, such as carbon steels (e.g., while an aqueous detergent solution may be appropriate for stainless steels, it would not be for carbon steels where attack may take place). Prior to implementing a cleaning procedure, it must be demonstrated that in addition to removing surface contamination, the technique does not adversely impact the surface of the test specimen.

Coupon Dimensions: Coupons should be sized based upon the anticipated rate of attack and test duration. While a high surface area to volume ratio is desirable for corrosion resistant materials, such as stainless steels, this is not the case for corrosion allowance materials such as carbon steel, where complete consumption of the test coupon could take place, or coupon dimensions altered to the extent that calculation of an accurate corrosion rate is hindered. Once sized, the dimensions of each coupon should be documented using a calibrated measurement device. Replicate measurements should be made to minimize measurement uncertainty. The accuracy of the measurements is important, as they will be used to calculate the surface area of the coupons in order to convert mass loss to a corrosion rate.

Weight measurement: As with dimensional measurements, a calibrated scale with a suitable accuracy should be used. It should be noted that balances are generally calibrated for linearity and eccentricity, but not accuracy. Separate mass standards are used to provide the calibration for accuracy at the time of measurement. An appropriate procedure was developed for the evaluation of weight loss coupons from the Long Term Corrosion Test Facility under the Yucca Mountain Project. This procedure (TST-PRO-T-006: *Sample Weighing Procedure Using an Electronic Analytical Balance*) describes a modified single substitution technique, and ensures that the measurement uncertainty will be minimized.   This procedure was developed during the performance of long-term corrosion testing associated with the long-term corrosion test facility for the Yucca Mountain Project. The procedure is based upon the National Institute of Standards and Technology (NIST) Standard Operating Procedure (SOP) No. 7: *Recommended Standard Operations Procedure for Weighing by Single Substitution Using a Single-Pan Mechanical Balance, a Full Electronic Balance, or a Balance with Digital Indications and Built-In Weights* (NIST, 2012), which is also an appropriate methodology.

Descaling methodology: A descaling solution is designed to remove the corrosion product present on the sample surface post-test. While ideally the solution would not attack the underlying base metal, some corrosion is inevitable. As such, the method through which the descaling solution is used must be able to resolve which portion of the weight change is due to corrosion product removal, and what is due to removal of base metal. By performing repeated cleaning cycles, followed by measurement of the sample mass, it is possible to observe when the corrosion product has been removed, as well as the rate at which the underlying substrate is being attacked, such that the latter may be deconvoluted from the former. Both the procedure, as well as potential descaling solutions for a variety of materials, are presented in ASTM G1. The descaling solutions outlined in the ASTM specification provide examples that will tend to dissolve the corrosion product, but protect exposed metal via a corrosion inhibitor. Such a solution is important in the case of corrosion-allowance materials such as carbon steel, where the corrosion rates in the uninhibited cleaning solution could be substantial. Prior to employing this method on actual test specimens, the effectiveness of the selected descaling solution must be demonstrated and documented.

Weight loss determination: The weight loss is calculated via simple subtraction of the corrected, descaled coupon weight from the initial coupon weight. As discussed in Section 2.2.2.2 above, once the weight loss of a test coupon has been determined, the average depth of attack can then be calculated as $\Delta W/(SA*\rho)$, where ΔW is the weight change, SA is the surface area of the coupon (calculated from the initial dimensional data), and ρ is the density of the material. This average depth of attack can be turned into a corrosion rate by dividing by the time period of the test.. It should be noted that conversion of the weight loss to a general corrosion rate requires that the nature of the observed attack be general in nature. If significant localized attack has taken place, an equivalent general corrosion rate can still be calculated, but its accuracy is substantially reduced, and as such should only be used as a qualitative indication of the corrosion rate, rather than a quantitative measure.

3.3.3   Corrosion of Carbon Steel

As discussed in Section 3.1, the carbon steel coupons for the tasks described below will conform to ASTM A216, Grade WCA. While the corrosion performance of corrosion resistant materials can be strongly impacted by welding, this effect is small for carbon steel. As such, the carbon steel coupons for the tasks outlined in this test plan will be not be welded.

3.3.3.1   *Task 1: Low Mg^{2+} Concentration Brine*

The purpose of this task is to develop an understanding of the corrosion properties of the carbon steel overpack in a relevant anoxic, low Mg^{2+} concentration brine, in light of the apparent inconsistency/variability presented in the literature. One of the concerns which has been revealed upon assessing the available literature is the large degree of scatter which exists in the corrosion rates, both within individual studies, as well as when comparing the results of one researcher to another. In addition, while some studies have suggested that corrosion rates will decline with time (Westerman et al., 1988), others indicate that the corrosion rates will reach a stable, steady state corrosion rate with time (Kursten, 2004). Care will be taken to prepare the samples in the same manner, both in terms of the cleaning processes applied as well as the surface finish imparted on the coupons prior to exposure, as described in Section 3.3.2 above.

Furthermore, analysis techniques will be carefully controlled, such that errors due to measurement uncertainty are minimized.

The brine selected for this evaluation is the PBB2 brine also used by Westerman et al. (1988). The behavior will be evaluated both in the bulk brine, as well as within a brine/salt mixture. The brine/salt ratio will be high enough that the reactions will not be brine-limited during the test intervals. Following the procedure of Westerman et al. (1988) for a test with 20 or 30 wt % H_2O, brine should be added to the test vessel after the coupons are embedded in a measured amount of dried NaCl.

Long-term immersion tests will be performed in an autoclave or similar construct, such that the environment can be maintained at the necessary combination of temperature and pressure. Samples will be placed within the test vessel, electrically isolated from one another as well as the chamber itself (if the selected chamber is metallic in nature). Measured amounts of brine, or salt and brine, will be added to the test vessel. The test vessel will be sized such that corrosion of the test coupons does not impact the bulk environment, such as the magnesium concentration. However, the hydrogen concentration, pH, and Fe^{2+} concentration are expected to be impacted. For the salt/brine mixture tests, different test vessels will be used for each combination of brine/temperature/exposure time. For the brine-only tests, samples for more than one time interval may be put into the same test vessel. In addition, it is desirable to split the coupons into two separate containers for each set of test conditions, such that an experimental issue with one does not eliminate all data for a particular test condition. Specimens will be removed after specific time periods for analysis of weight loss as well as to evaluate the composition of the corrosion products as a function of time. In addition, the composition of the brine itself will be evaluated upon the completion of each test interval. If test vessels are populated such that multiple time intervals are present in the same vessel, then extreme care must be taken to prevent oxygen contamination of the test vessel. The vessel must be opened in oxygen free conditions, such as within a glove box, and resealed in that same environment. While opening the vessel will result in a loss of any corrosion generated hydrogen, this is not anticipated to have a measureable impact on the corrosion rate, as revealed by Telander and Westerman (1997).

3.3.3.2   Task 2: High Mg^{2+} Concentration Brine

The purpose of this task is to develop an understanding of the corrosion properties of the carbon steel overpack in a relevant anoxic, high Mg^{2+} concentration brine, in light of the apparent inconsistency/variability presented in the literature. As discussed above, one of the concerns which has been revealed upon assessing the available literature is the large degree of scatter which exists in the corrosion rates, both within individual studies, as well as when comparing the results of one researcher to another. In addition, while some studies have suggested that corrosion rates will decline with time (Westerman et al., 1988), others indicate that the corrosion rates will reach a stable, steady state corrosion rate with time (Kursten, 2004). Care will be taken to prepare the samples in the same manner, both in terms of the cleaning processes applied as well as the surface finish imparted on the coupons prior to exposure, as described in Section 3.3.2 above. Furthermore, analysis techniques will be carefully controlled, such that errors due to measurement uncertainty are minimized.

The brine selected for this evaluation is the WIPP Brine A. Considerable experimental data exists already for materials in this particular environment, providing a large quantity of data which can be used to validate, in part, the results obtained in this study.   The behavior will be evaluated both in the bulk brine, as well as within a brine/salt mixture. The brine/salt ratio will be high enough that the reactions will not be brine-limited during the test intervals. Following the procedure of Westerman et al. (1988) for a test with 20 or 30 wt % H_2O, brine should be added to the test vessel after the coupons are embedded in a measured amount of dried NaCl.

As in Task 1, long-term immersion tests will be performed in an autoclave or similar construct, such that the environment can be maintained at the necessary combination of temperature and pressure. Samples will be placed within the test vessel, electrically isolated from one another as well as the chamber itself (if the selected chamber is metallic in nature).   Measured amounts of brine, or salt and brine, will be added to the test vessel. The test vessel will be sized such that corrosion of the test coupons does not impact the bulk environment, such as the magnesium concentration. However, the hydrogen concentration, pH, and Fe^{2+} concentration are expected to be impacted.   For the salt/brine mixture tests, different test vessels will be used for each combination of brine/temperature/exposure time. For the brine-only tests, samples for more than one time interval may be put into the same test vessel.   In addition, it is desirable to split the coupons into two separate containers for each test conditions, such that an experimental issue with one does not eliminate all data for a particular test condition. Specimens will be removed after specific time periods for analysis of weight loss as well as to evaluate the composition of the corrosion products as a function of time. In addition, the composition of the brine itself will be evaluated upon the completion of each test interval. If test vessels are populated such that multiple time intervals are present in the same vessel, then extreme care must be taken to prevent oxygen contamination of the test vessel. The vessel must be opened in oxygen free conditions, such as within a glove box, and resealed in that same environment. While opening the vessel will result in a loss of any corrosion generated hydrogen, this is not anticipated to have a measureable impact on the corrosion rate, as revealed by Telander and Westerman (1997).

3.3.3.3 Task 3: Corrosion Product Identification as a Function of Time and Environment

The purpose of this task is to identify the nature of the corrosion products which form when carbon steel is exposed to the high and low Mg^{2+} concentration brines described in Task 1 and 2.

As the corrosion products will be produced under anoxic conditions, it is critical that exposure of the corrosion product to oxygen be avoided. Test vessels should be opened within a glove box or bag containing an inert, deoxygenated environment such as nitrogen or argon. Once removed, the corrosion product must be stored in such conditions until analysis is complete.

If sufficient corrosion product is available, the identity will be determined by XRD and the composition will be determined by chemical analysis.   The selected methods for chemical analysis will depend on the capabilities of the lab where the work is performed. The accuracy and capability of the selected techniques must be demonstrated and documented prior to the analysis of any actual test coupons.

Isolation of the corrosion product from the test samples must be done in a manner such that no additional contamination of the corrosion product takes place. Thus, whatever tools are used to scrape or otherwise extract the corrosion product from the test coupon surface must not be friable such that they contribute to the corrosion product.

When there are only thin layers of corrosion products, the surface of the coupons will be examined by SEM combined with EDS.

In addition to the experimental work proposed, first-principles modeling using density functional theory (DFT) will be carried out to predict and help establish the identity of the corrosion products analyzed using XRD. DFT has been successfully used to obtain crystal structures that match XRD patterns of numerous metal oxides and hydroxides (see e.g. Lavina et al., 2011, and Weck et al., 2012). DFT can palliate some of the shortcomings of XRD, such as the notorious inability of XRD techniques to determine the position of hydrogen atoms within compounds or to systematically and unambiguously establish the space groups of crystalline structures; both of these difficulties can be overcome with total-energy calculations using DFT.

3.3.4   Corrosion of Stainless Steel

As discussed in Section 3.1, 304L SS (UNS S30403) will be the material evaluated in the tasks described below. To eliminate potential variations in performance due to thermal processing, the 304SS will be in the annealed condition per ASTM A480. For task 4, the carbon steel will again conform to ASTM A216, Grade WCA. Since the stainless steel is a low carbon containing alloy, weld sensitization is not anticipated, and therefore the coupons will be evaluated in the annealed, unwelded condition.

3.3.4.1   Task 4: Characterization of the Environment at the Stainless Steel/Carbon Steel Corrosion Product Interface for high and low Mg^{2+} concentration Brines

As discussed in Section 2.3.4, the environment at the surface of the stainless steel upon breach of the carbon steel overpack, while it will be a function of the local brine composition, will also include significant contributions from the carbon steel corrosion products which will separate the bulk salt from the stainless steel. In order to effectively assess the corrosion performance of the stainless steel liner within a salt repository, this local environment must be determined.

Two approaches will be used to assess this environment – one theoretical, and one experimental. The theoretical approach will include thermodynamic modeling of the brines using EQ3/6 (Wolery et al., 2010). While thermodynamic data for the major brine constituents are available for 25⁰C, there are many gaps in data for minor constituents like Fe^{2+} and for higher temperatures. Xiong et al. (2012) have a plan to close these gaps, and any modeling work should be done in close coordination with that work. The plan of Xiong et al. includes measuring the solubility of the corrosion products identified in Task 3. Modeled brine compositions will be compared to the bulk brine compositions measured in Tasks 1 and 2.

In addition to the theoretical approach, an effort will be made to experimentally extract and characterize the liquid brine which exists within the corrosion product layer produced during experiments nominally identical to the salt+brine experiments defined in Tasks 1 and 2. Carbon steel coupons will be prepared and placed into a test vessel similar to that done in the aforementioned tasks. Upon extraction of the corrosion product, an effort will be made to remove the liquid phase from the corrosion product via vacuum extraction or a similar method. If suitable quantities of brine cannot be extracted, aqueous extraction using small quantities of deionized water will be attempted. Chemical analysis of the brines will be performed at several time intervals, such that the evolution of the brine over time can be determined. As a large quantity of corrosion product will be necessary for the extraction, the corrosion coupons used for this test should be in addition to those described in Tasks 1 and 2, to ensure a sufficient volume of material is available for replicate measurements. The chemistry of the brine within the corrosion products will be compared to that of the bulk brine within the tests.

3.3.4.2   Task 5: General and Localized Corrosion Performance of Stainless Steel in The Environment Determined in Task 4.

Once the appropriate test environments at the stainless steel surface have been identified, the general and localized corrosion performance of the stainless steel will be assessed. Both long-term exposure testing, as well as instrumented electrochemical testing will be performed to assess the localized corrosion resistance of the stainless steel.

Cyclic potentiodynamic polarization (CPP) will be performed to assess the pitting and repassivation behavior of the stainless steel. Once formulated, the brines will be deaerated before use and N_2 will be purged through the solutions for at least 24 hours. During purging, the corrosion potential (E_{CORR}) will be measured using a calibrated reference electrode. A silver/silver chloride reference electrode will be used (for its elevated temperature stability) attached to the main exposure cell via a Luggin probe that maintains the electrode at ambient temperature, and a platinum counter electrode (foil or rod) will be used. After E_{CORR} has been determined, CPP tests will be performed in accordance with ASTM G 61-86, *Standard Test Method for Conducting Cyclic Potentiodynamic Polarization Measurements for Localized Corrosion Susceptibility of Iron-, Nickel-, or Cobalt-Based Alloys*. A calibrated potentiostat/galvanostat will be used that has a sufficient current resolution to capture behavior at the passive current density as well as upon the initiation of localized corrosion. Polarization scans will be initiated at a potential 150 mV cathodic of the corrosion potential, then scanned at a rate of 0.167mV/s until pitting or transpassive dissolution occurs, and the current density reaches 5 mA/cm^2. At that point, the scan will be reversed and continued at least until the repassivation potential has been reached.

In addition to the electrochemical testing, samples will be prepared and immersed in the brine established in Task 4. Testing will mimic that of Tasks 1 and 2. Upon the removal of each sample, the number density and depth of any localized attack will be documented, as well as the weight change observed over time. Where possible, cross sectional analyses will be performed to determine the approximate depth of representative localized corrosion sites. It should be noted that if localized attack has taken place, it will not be possible to reliably convert the weight

loss to a general corrosion rate. However the weight loss data can be used to provide a net corrosion rate, which can be used to calculate H_2 generation rates in TSPA calculations.

3.3.4.3   Task 6: Corrosion product identification as a function of time and exposure environment

The purpose of this task is to identify the nature of the corrosion products which form when stainless steel is exposed to the brines determined in Task 4. Like Task 3, the corrosion products must be protected from the air (i.e., oxygen) to prevent oxidation. It is expected that the amount of corrosion product formed will be less than that in the carbon steel tests, so XRD and chemical analysis may not be possible. In this case, SEM combined with EDS will be used to investigate the corrosion products in several locations, including areas of localized and general corrosion.

3.4   Test Matrix

The following test matrix is for 2 years. However, for the time dependence of the corrosion rates, longer test intervals are desired. In addition, for some test conditions, there may not be enough corrosion products for identification after 2 years. Therefore it is prudent to include the possibility for testing to continue after 2 years in the design and set up of the experiments.

There are two types of test conditions in the test matrix, brine-only and brine/salt mixture. The brine-only tests will be performed because they have a larger quantity of brine that is easy to extract and characterize. The brine/salt mixture tests will be performed because the salt holds the corrosion products against the samples much like the salt will hold the corrosion products against the waste packages, which may influence the long-term corrosion rates. For an example of experimental set up using salt/brine mixtures see Westerman et al. 1986 and 1988.   If initial test development tests show that a brine reservoir within the brine/salt tests communicates well with the brine at the coupon surface, and if brine in this reservoir may be easily sampled, then the brine-only tests would become unnecessary.

The tables below show the minimum number of test coupons that are needed assuming that separate samples are required for weight loss and corrosion product identification. However, when the corrosion product layers are thick, it may be possible to obtain corrosion product samples from the weight loss coupons prior to cleaning, thus reducing the number of coupons needed. In addition, in the brine-only tests, coupons for more than one time interval may be loaded into the test vessels, provided that the time the vessel is open is minimized, any fluids withdrawn are replenished, and the vessel is opened in oxygen free conditions, such as within a glove box, and resealed in that same environment.

.

3.4.1   Corrosion of Carbon Steel

3.4.1.1   Task 1: Low Mg^{2+} Concentration Brine

Tables 3-4 and 3-5 below describe the minimum number of test coupons which should be evaluated at each test condition. In addition to evaluating the test coupons, the composition of the brine must be evaluated upon the completion of each test interval, such that any deviations which occur as a function of time are documented.

Table 3-4. Experiments in PBB2 Brine

	30°C		90°C		150°C	
	Weight Loss	Corrosion Product	Weight Loss	Corrosion Product	Weight Loss	Corrosion Product
1 Month	3	2	3	2	3	2
6 Months	3	2	3	2	3	2
12 Months	3	2	3	2	3	2
24 Months	3	2	3	2	3	2

Table 3-5. Experiments in PBB2 Brine + NaCl

	30°C		90°C		150°C	
	Weight Loss	Corrosion Product	Weight Loss	Corrosion Product	Weight Loss	Corrosion Product
1 Month	7	3	7	3	7	3
6 Months	7	3	7	3	7	3
12 Months	7	3	7	3	7	3
24 Months	7	3	7	3	7	3

3.4.1.2   Task 2: High Mg^{2+} Concentration Brine

Tables 3-6 and 3-7 below describe the minimum number of test coupons which should be evaluated at each test condition. In addition to evaluating the test coupons, the composition of the brine must be evaluated upon the completion of each test interval, such that any deviations which occur as a function of time are documented.

Table 3-6. Experiments in Brine A

	30°C		90°C		150°C	
	Weight Loss	Corrosion Product	Weight Loss	Corrosion Product	Weight Loss	Corrosion Product
1 Month	3	2	3	2	3	2
6 Months	3	2	3	2	3	2
12 Months	3	2	3	2	3	2
24 Months	3	2	3	2	3	2

Table 3-7. Experiments in Brine A + NaCl

	30°C		90°C		150°C	
	Weight Loss	Corrosion Product	Weight Loss	Corrosion Product	Weight Loss	Corrosion Product
1 Month	7	3	7	3	7	3
6 Months	7	3	7	3	7	3
12 Months	7	3	7	3	7	3
24 Months	7	3	7	3	7	3

3.4.1.3   Task 3: Corrosion Product Identification as a Function of Time and Environment

Test matrix defined by Tasks 1 and 2. If enough corrosion products are available, samples will be subdivided such that at least three replicate measurements can be made to the corrosion products from each test coupon. The average composition, as well as the standard deviation, will be reported as appropriate.

3.4.2   Corrosion of Stainless Steel

3.4.2.1   Task 4: Characterization of the Environment at the Stainless Steel/Carbon Steel Corrosion Product Interface for high and low Mg^{2+} concentration Brines

As discussed in Section 3.3.4.1, Task 4 will determine the brine chemistry within the growing corrosion product layer on corroding carbons steel. Table 3-8 below describes the minimum number of test coupons which should be evaluated at each test condition and time period. However, predictions of the amount of corrosion products generated for each condition and time period should be made prior to opening the test vessels. When insufficient corrosion product is

predicted for brine extraction, the test vessel will not be opened. Tests beforehand should be conducted to determine the minimum amount of corrosion product needed to collect a brine sample.   If the system setup allows bulk brine sampling without opening the vessel, such sampling should be made shall be made at the intervals shown in Table 3-8.

Table 3-8. Experiments for Corrosion Product Brine Extraction from Brine+Salt Mixture Tests

	30°C		90°C		150°C	
	Brine A	**PBB2**	**Brine A**	**PBB2**	**Brine A**	**PBB2**
1 Month	3	3	3	3	3	3
6 Months	3	3	3	3	3	3
12 Months	3	3	3	3	3	3
24 Months	3	3	3	3	3	3

3.4.2.2   Task 5: General and Localized Corrosion Performance of Stainless Steel in The Environment Anticipated from Task 4.

Table 3-9 below describes the minimum number of test coupons which should be evaluated at each test condition. The brine chemistries are identified in terms of the bulk brine, but will be the brine which forms within the carbon steel corrosion products for each of the test conditions. The table is applicable to both the electrochemical testing to determine critical potentials, as well as the long-term immersion testing to determine mass loss vs. time as well as the number density and size of localized corrosion sites.

Table 3-9. Experiments for Determination of Localized Corrosion Performance of Stainless Steel in Brine

	30°C		90°C		150°C	
	Brine A	**PBB2**	**Brine A**	**PBB2**	**Brine A**	**PBB2**
1 Month	3	3	3	3	3	3
6 Months	3	3	3	3	3	3
12 Months	3	3	3	3	3	3
24 Months	3	3	3	3	3	3

3.4.2.3   Task 6: Corrosion product identification as a function of time and exposure environment.

Test matrix defined by Task 5. If enough corrosion products are available, samples will be subdivided such that at least three replicate measurements can be made to the corrosion products from each test coupon. In order to accomplish this, the corrosion products from multiple localized corrosion sites will need to be assessed. It should be noted that if appreciable general corrosion has taken place, the corrosion products at the surfaces where localized attack has not taken place should be assessed separately from regions where a pit has nucleated and grown. The average composition, as well as the standard deviation, will be reported as appropriate.

4.   IMPLEMENTING DOCUMENTS

4.1   Implementing Procedures

The implementing procedures that will be used to conduct the science activities described in Sections 2.1 through 2.3 are listed below. These procedures may be updated during the course of the testing covered by this technical work plan (TWP). When a procedure is updated, it is the responsibility of the principal investigator performing the work to correctly identify the revised procedure in the appropriate locations in the scientific notebook and to evaluate the revised procedure in terms of meeting the testing goals. If a formal procedure does not exist for a particular activity, or an industry standard is utilized to govern the test protocol, the methodology, test parameters, etc. will be described in detail in the scientific notebook. Where test parameters or approaches differ from a previously documented procedure, the testing will be described in sufficient detail in the scientific notebook such that the test can be reproduced by a person knowledgeable in the area of corrosion science and testing.

- Fuel Cycle Technologies (FCT) Quality Assurance Program Document, Rev. 1 (DOE, 2011)

- TST-PRO-T-006: *Sample Weighing Procedure Using an Electronic Analytical Balance* (BSC, 2008): This procedure was developed during the performance of long-term corrosion testing associated with the long-term corrosion test facility for the Yucca Mountain Project. It is based upon the National Institute of Standards and Technology (NIST) Standard Operating Procedure (SOP) No. 7: *Recommended Standard Operations Procedure for Weighing by Single Substitution Using a Single-Pan Mechanical Balance, a Full Electronic Balance, or a Balance with Digital Indications and Built-In Weights* (NIST, 2012).

4.2   Directly Applicable Specifications

Work will conform, as appropriate, to guidance provided in the ASTM standards listed below. Not all test activities will implement all facets of the standards listed below. Where test parameters or approaches differ from the listed standards, the testing will be described in sufficient detail in the scientific notebook such that the test can be reproduced by a person knowledgeable in the area of corrosion science and testing.

- ASTM A216-08, *Standard Specification for Steel Castings, Carbon, Suitable for Fusion Welding, for High-Temperature Service.*

- ASTM A240-06, *Standard Specification for Chromium and Chromium-Nickel Stainless Steel Plate, Sheet, and Strip for Pressure Vessels and for General Applications.*

- ASTM A480-12, *Standard Specification for General Requirements for Flat-Rolled Stainless and Heat- Resisting Steel Plate, Sheet, and Strip*

- ASTM A516-06, *Standard Specification for Pressure Vessel Plates, Carbon Steel, for Moderate and Lower Temperature Service.*

- ASTM G1-03, *Standard Practice for Preparing, Cleaning, and Evaluating Corrosion Test Specimens*

- ASTM G 61-86, *Standard Test Method for Conducting Cyclic Potentiodynamic Polarization Measurements for Localized Corrosion Susceptibility of Iron-, Nickel-, or Cobalt-Based Alloys.*

5.   TEST EQUIPMENT AND CALIBRATION

Testing activities will use standard test equipment and the details for specific test equipment will be documented in the activity-specific scientific notebook, summary report, or other appropriate media.

A list of chemicals required for corrosion testing and analysis is given in Table 5-1. If chemicals are used that are not included in Table 5-1, an appropriate notation will be made in the scientific notebook. The preferred purity for chemical reagents is American Chemical Society (ACS)-grade purity from commercial suppliers. If ACS-grade purity is not available or a different purity level is required by the principal investigator, the purity level selected will be justified in the scientific notebook. All chemicals used as standards will require traceability to the National Institute of Standards and Technology (NIST).

For corrosion testing, standard material and corrosion Measurement and Testing Equipment (M&TE) will be used and calibration requirements shall be documented in accordance with applicable procedures. The activity-specific scientific notebook shall contain the proper documentation for M&TE. A list of M&TE to be used is given in Table 5-2, together with the frequency of calibration and applicable calibration/use procedures. The first entry for new M&TE in the scientific notebook will describe the intended use of the equipment, and the required calibration frequency and type of calibration (e.g., time of use, Sandia National Laboratories (SNL) Primary Standards Laboratory, etc.).

For solution chemistry and corrosion product identification, a variety of different techniques may be appropriate, and the techniques employed will depend on the procedures available at the lab where the work is performed. As such, these techniques are not specifically called out in the table below. The calibration method used for any technique will be identified and documented prior to the performance of any experimental work.

Table 5-1. Chemicals Used for Testing and Analysis

Chemical	Formula	Use
Sodium Chloride	NaCl	Brine synthesis
Calcium chloride dihydrate	$CaCl_2 \cdot 2H_2O$	Brine synthesis
Magnesium chloride hexahydrate	$MgCl_2 \cdot 6H_2O$	Brine synthesis
Sodium Sulfate	Na_2SO_4	Brine synthesis
Sodium tetraborate decahydrate	$Na_2B_4O_7 \cdot 10H_2O$	Brine synthesis
Sodium hydrogen carbonate (sodium bicarbonate)	$NaHCO_3$	Brine synthesis
Potassium chloride	KCl	Brine synthesis
Hydrochloric acid	HCl	Brine synthesis, Chemical Analysis
Sodium hydroxide	NaOH	Brine synthesis
pH buffers	pH 2, 4, 7, 10, 11	pH calibration

Table 5-2. M&TE Calibration Frequency

Potentiostat/Galvanostat	Once per year or if operation suspect	Per manufacturers procedure
Weight set	Once every 5 years or if operation suspect/surface contaminated	SNL Primary Standards Lab or the equivalent
Digital scale	Once per year or if operation suspect	SNL Primary Standards Lab or the equivalent
Digital calipers	Time of use	Measuring blocks (see below)
Measuring blocks	Once per year or if operation suspect	SNL Primary Standards Lab or the equivalent
Thermocouples	Once per year or if operation suspect	SNL Primary Standards Lab or the equivalent

6.   RECORDS

Required records will be developed, maintained, collected, compiled, and submitted in accordance with the records management procedures at the laboratory where the work takes place.

Anticipated records may include the scientific notebooks, M&TE calibrations, chemical certifications, test material certifications, electronic data files (e.g., polarization data, open circuit data, images, chemical analysis), and results of assessments and readiness reviews.

7.   TRAINING AND QUALIFICATION

Personnel conducting work under this TWP must be trained to the relevant procedures governing this work. Additionally, site- and organization-specific training requirements must be met. Topics anticipated to be covered by this training will include, but are not limited to, Environmental, Safety and Health roles and responsibilities; hazard awareness and emergency response; organization requirements for work planning; working with hazardous chemicals; and safe operation of lab equipment and associated facilities.

8.   SOFTWARE

Commercial off-the-shelf software will be used in the collection and interpretation of these experimental data. The aqueous speciation and solubility program EQ3/6 (V. 8.0a, Wolery et al., 2010) will be used for thermodynamic modeling calculations. Spin-polarized density functional theory calculations to characterize the structures and properties of the corrosion products will be carried out using the Vienna ab initio simulation package (VASP) (Kresse and Furthmüller, 1996).

9.   PROCUREMENT

The items and services that may be procured to support the testing activities described in this TWP include:

- Equipment calibration and servicing
- Chemicals
- Analytical services
- Subcontract testing services.

All procurements will be made via normal channels for the laboratory at which the experimentation takes place, following the appropriate corporate regulations.

10. REFERENCES

Anderson, G.M., and R.W. Macqueen. 1982. Ore deposit models - 6. Mississippi Valley-Type lead-zinc deposits. Geoscience Canada 9, 108-117.

ASTM A216/A216M. 2008. Standard Specification for Steel Castings, Carbon, Suitable for Fusion Welding, for High-Temperature Service. American Society for Testing and Materials, West Conshohocken, Pennsylvania.

ASTM A240/A240M. 2006. Standard Specification for Chromium and Chromium-Nickel Stainless Steel Plate, Sheet, and Strip for Pressure Vessels and for General Applications. American Society for Testing and Materials, West Conshohocken, Pennsylvania.

ASTM A480/A480M, 2012. Standard Specification for General Requirements for Flat-Rolled Stainless and Heat- Resisting Steel Plate, Sheet, and Strip. American Society for Testing and Materials, West Conshohocken, Pennsylvania.

ASTM A516/A516M. 2006. Standard Specification for Pressure Vessel Plates, Carbon Steel, for Moderate and Lower Temperature Service. American Society for Testing and Materials, West Conshohocken, Pennsylvania.

ASTM G1. 2011. Standard Practice for Preparing, Cleaning, and Evaluating Corrosion Test Specimens. American Society for Testing and Materials, West Conshohocken, Pennsylvania.

ASTM G61-86. 2009. Standard Test Method for Conducting Cyclic Potentiodynamic Polarization Measurements for Localized Corrosion Susceptibility of Iron-, Nickel-, or Cobalt-Based Alloys. American Society for Testing and Materials, West Conshohocken, Pennsylvania.

Braithwaite, J. W. and M.A. Molecke. 1980. Nuclear Waste Canister Corrosion Studies Pertinent to Geologic Isolation, *Nuclear and Chemical Waste Management*, *1*(1), 37-50.

Brush, L. 1995. *Systems Prioritization Method Iteration 2, Baseline Position Paper: Gas Generation in the Waste Isolation Pilot Plant.* Albuquerque: Sandia National Laboratories.

Brush, L.H. 2005. *Results of Calculations of Actinide Solubilities for the WIPP Performance Assessment Baseline Calculations*. Analysis report, May 18, 2005. Carlsbad, NM: Sandia National Laboratories. ERMS 539800.

Bryan, C.R., D.G. Enos, L. Brush, A. Miller, K. Norman, and N.R. Brown. 2011. *Engineered Materials Performance: Gap Analysis and Status of Existing Work*. FCRD-USED-2011-000407. SAND 2011-7896P. Albuquerque, NM: Sandia National Laboratories.

BSC. 2004. *Aqueous Corrosion Rates for Waste Package Materials.* ANL-DSD-MD-000001 REV 01, Bechtel SAIC Co. LLC, Las Vegas, Nevada.

BSC. 2008. *Sample Weighing Procedure Using an Electronic Analytical Balance.* TST-PRO-T-006: Bechtel SAIC Co. LLC, Las Vegas, Nevada.

Carter, J.P. and F.X. McCawley. 1982. "*Corrosion Tests in Brine and Steam from the Salton Sea KGRA*", J. Materials for Energy Systems, Vol. 3, No. 4 (March, 1982), pp.30-38.

Chivot, J. 2004. Thermodynamique des produits de corrosion: Fonctions thermodynamiques, diagrammes de solubilité, diagrammes E-pH des systèmes Fe-H2O, Fe-CO2-H2O, Fe S H2O, Cr-H2O, et Ni-H2O en fonction de la température. *Collection sciences et techniques.* Châtenay-Malabry, France:Agence National pour la Gestion des Déchets Radioactifs.

Cramer, S.D. and J.P. Carter. 1980. "*Corrosion in Geothermal Brines of the Salton Sea Known Geothermal Resource Area*", ASTM STP 707, Geothermal Scaling and Corrosion, L.A.Casper, T.R. Pinchback, Eds., 1980, pp. 113-141.

Dean, W. E. and A.L. Tung. 1974. Trace and minor elements in anhydrite and halite, Supai Formation (Permian), east-central Arizona. Proceedings of the 4th Symposium on Salt, p. 75-285. Cleveland:Northern Ohio Geological Society.

De Las Cuevas, C. and J.J. Pueyo. 1995. The influence of mineralogy and texture in the water content of rock salt formations. Its implication in radioactive waste disposal. *Applied Geochemistry* **10**(3)**,** 317-327.

DOE. 2007. *Fall 2006 Assessment of Matheson Wetlands Hydrogelogy and Ground Water Chemistry.* DOE-EM/GJ1441-2007, Grand Junction, CO: U.S. Department of Energy Office of Environmental Management.

DOE. 2011. Fuel Cycle Technologies Quality Assurance Program Document, Rev.1. DOE Office of Fuel Cycle Technologies, NE-5. Washington, DC.

Dombrowski, H. 1963. *Bacteria from Paleozoic salt deposits*. Annals of the New York Academy of Sciences, v. 108, p 453–460.

Emons, H., and T. Fanghaenel. 1989. Thermal Decomposition of Carnallite (KCl.MgCl2.6H2O) - Comparisom of Experimental Results and Phase Equilibria. *Journal of Thermal Analysis, 35*, 2161-2167.

Hansen, F.D., and C.D.Leigh. 2011. *Salt Disposal of Heat-Generating Nuclear Waste*. SAND2011-0161. Albuquerque: Sandia National Laboratories.

Heydari, E., and C.H. Moore. 1989. Burial diagenesis and thermochemical sulfate reduction, Smackover Formation, southeastern Mississippi salt basin. Geology 17, 1080-1084.

Hoerle, S., F. Mazaudier, P. Dillmann, and G. Santarini. 2004. Advances in Understanding Atmospheric Corrosion of Iron. II. Mechanistic Modelling of Wet-Dry Cycles. *Corrosion Science, 46*, 1431-1465.

Holt, R.M., and D.W. Powers. 2011. Synsedimentary dissolution pipes and the isolation of anceinet bacteria and cellulose. Geological Society of America bulletin, Vol. 123, Issue 7-8, 1513-1523.

ISO 8407. 2009. Corrosion of Metals and Alloys: Removal of Corrosion Products from Corrosion Test Specimens, 2nd Edition. International Organization for Standardization, Geneva, Switzerland.

Jockwer, N. 1981. Laboratory investigations of water content within rock salt and its behavior in a temperature field of disposed high level waste. *In:* Moore, J. G. (ed.) *Scientific Basis for Nuclear Waste Management, Proceedings of the Third International Symposium on the Scientific Basis for Nuclear Waste Management, as part of the Annual Meeting of the Materials Research Society.* **3**. New York, NY: Plenum Press. 35-40.

Knauth, L.P. and M.B. Kumar. 1981. Trace water content in Louisiana salt domes. *Science* **213**(4511)**,** 1005-1007.

Kresse, G. and J. Furthmuller. 1996. Efficient iterative schemes for ab initio total-energy calculations using a plane-wave basis set. *Physical Review B: Condens. Matter Mater. Phys.* **54,** 11169-11186.

Kursten, B., E. Smailos, I. Azkarate, L. Werme, N.R. Smart, and G. Santarini. 2004. *COBECOMA: State-of-the-art document on the COrrosion BEhaviour of COntainer MAterials. European Commission 5th Euratom Framework Programme, 1998-2002*. Contract no. FIKW-CT-20014-20138 Final Report: European Commission.

Lappin, A., R. Hunter, D. Garber, and P. Davies. 1989. *Systems Analysis, Long-Term Radionuclide Transport, and Dose Assessments, Waste Isolation Pilot Plant (WIPP), Southeastern New Mexico.* SAND89-0462, Albuquerque: Sandia National Laboratories.

Lavina B., P. Dera, E. Kim, Y. Meng, R.T. Downs, P.F. Weck, S.R. Sutton, Y. Zhao. 2011. Discovery of the recoverable high-pressure iron oxide Fe_4O_5. *Proc. Natl. Acad. Sci. USA* **108**, 17281-17285.

Lowenstein, T.K., B.A. Schubert, and M.N. Timofeeff. 2011. *Microbial communities in fluid inclusions and long-term survival in halite.* GSA Today, v. 21, no. 1, pp. 4-9.

MacDonald, D.D., B.C. Syrett, and S.S. Wing. 1979. *The Use of Potential-pH Diagrams for the Interpretation of Corrosion Phenomena in High Salinity Geothermal Brines.* Corrosion. Vol. 35. No. 1, pp 1-11. NACE, Houston Texas.

Machel, H.G. 2001. "Bacterial and thermochemical sulfate reduction in diagenetic settings – old and new insights". *Sedimentary Geology 140*, 143-175.

Mayhew, E. J. and E.B. Heylmun. 1966. Complex salt and brines of the Paradox Basin, in Proceedings of the 2nd Symposium on Salt, p. 221-235. Cleveland: Northern Ohio Geological Society.

Mintz T.S., L. Caseres, X. He, J. Dante, G. Oberson, D.S. Dunn, and T. Ahn. 2012. *Atmospheric Salt Fog Testing to Evaluate Chloride-Induced Stress Corrosion Cracking of Type 304 Stainless Steel*. Corrosion 2012. Salt Lake City, Utah.

Molecke, M. A. 1983. *A Comparison of Brines Relevant to Nuclear Waste Experimentation.* SAND83-0516, Albuquerque, NM: Sandla National Laboratories.

Molecke, M.A.   1984. "Test Plan: Waste Package Performance Technology Experiments for Simulated DHLW". Sandia National Laboratories, Albuquerque, New Mexico.

Molecke, M. 1986a. *Memo of Record: Early Failure of Heaters in WIPP MIIT Brine Equilibration Hole.* Document WP02276, Albuquerque: Sandia National Laboratories.

Molecke, M. 1986b. *Memo of Record: Measurement of Hydrochloric Acid Vapors in WIPP from In Situ Experiments-Safety Aspects.* Document WP03146, Albuquerque: Sandia National Laboratories.

Molecke, M.A. and G.G. Wicks. 1992. "*Materials Interface Interactions Test (MIIT) Details and Observations on In Situ Sample Retrievals and Test Termination*", SAND92-1954C. Albuquerque, NM: Sandia National Laboratories.

NIST. 2012. SOP No. 7: *Recommended Standard Operations Procedure for Weighing by Single Substitution Using a Single-Pan Mechanical Balance, a Full Electronic Balance, or a Balance with Digital Indications and Built-In Weights.*   NIST. Gaithersburg, MD. *www.nist.gov/pml/wmd/labmetrology/upload/**SOP_7**_20120229.pdf*

Popielak, R.S., R.L. Beauheim, S.R. Black, W.E. Coons, C.T. Ellingson and R.L. Olsen. 1983. Brine Reservoirs in the Castile Formation, Waste Isolation Pilot Plant Project, Southeastern New Mexico. TME 3153. Carlsbad, NM: U.S. Department of Energy WIPP Project Office.

Pourbaix, M. 1974. Atlas of electrochemical equilibria in aqueous solutions. Houston, TX: NACE International.

Rai, D., A.R. Felmy, S.P. Juracich, and F. Rao. 1995. *Estimating the Hydrogen Ion Concentration in Concentrated NaCl and Na2SO4 Electrolytes*. SAND94-1949. Albuquerque, NM: Sandia National Laboratories.

Reiser, R., and P. Tasch. 1960. *Investigation of the viability of osmophile bacteria of great geological age.* Transactions of the Kansas Academy of Science, v. 63, p. 31–34.

Roedder, E. and R.L. Bassett. 1981. Problems in determination of the water content of rock salt samples and its significance in nuclear-waste storage siting. Geology **9**(11)**,** 525-530.

Roedder, E. and H.E. Belkin. 1979. Fluid inclusions in salt from the Rayburn and Vacherie Domes, Louisiana. Open-File Report no. 79-1675: U.S. Geological Survey.

Roosendaal, S., J. Bakker, A. Vredenberg, and F. Habraken. 2001. Passivation of Iron by Oxidation in H_2O and O_2/H_2O Mixtures. *Surface Science, 494*, 197-205.

Roselle, G.T. 2009. Iron and lead corrosion in WIPP-relevant conditions: Six month results. Milestone report, October 7, 2009. ERMS 546084, Carlsbad, NM: Sandia National Laboratories.

Roselle, G.T. 2010. Iron and lead corrosion in WIPP-relevant conditions: 12 Month Results. Milestone report, October 14, 2010. ERMS 554383, Carlsbad, NM: Sandia National Laboratories.

Roselle, G.T. 2011a. Iron and lead corrosion in WIPP-relevant conditions: 18 Month Results. Milestone report, January 5, 2011. ERMS 554715, Carlsbad, NM: Sandia National Laboratories.

Roselle, G.T. 2011b. Iron and lead corrosion in WIPP-relevant conditions: 24 Month Results. Milestone report, May 3, 2011. ERMS 555426, Carlsbad, NM: Sandia National Laboratories.

Roselle, G.T. 2012. SP 12-14, Use of pH meters and Electrodes, Revision 3. Sandia National Laboratories, Carlsbad, NM. https://nwmp.sandia.gov/onlinedocuments/nwmp/sp/sp1214.pdf

Rothfuchs, T. 1986. In situ investigations on the impact of heat production and gamma radiation with regard to high-level radioactive waste disposal in rock salt formations. *Nuclear Technology* **58,** 256-270.

Schikorr, G. 1933. Über Eisen(II)-hydroxyd und ein ferromagnetisches Eisen(III)-hydroxyd. *Zeitschrift für Anorganische und Allgemeine Chemie, 212*(1), 33-39.

Sevougian, S.D., G.A. Freeze, M.B. Gross, J. Lee, C.D. Leigh, P. Mariner, R.J. MacKinnon, and P. Vaughn. 2012. *TSPA Model Development and Sensitivity Analysis of Processes Affecting Performance of a Salt Repository for Disposal of Heat-Generating Nuclear Waste*. FCR&D-USED-2012-000320, Rev 0.

Shefelbine, H. C. 1982. *Brine Migration: A Summary Report*. SAND82-0152, Albuquerque, NM: Sandia National Laboratories.

Simpson, J., and R. Schenk. 1989. Corrosion Induced Hydrogen Evolution on High Level Waste Overpack Materials in Synthetic Groundwaters and Chloride Solutions. In W. Lutze, & R.

Ewing (Ed.), *Scientific Basis for Nuclear Waste Management XII, Berlin, Germany, October 10-13, 1988. 127*, pp. 389-396. Pittsburgh, PA: Materials Research Society Symposium Proceedings.

Smailos, E. 1993. "Corrosion of High-Level Waste Packaging Materials in Disposal Relevant Brines," Nuclear Technology, 104, pp. 343-350.

Smailos, E. 1999. "Corrosion behavior of selected HLW/spent fuel container materials under the conditions of the in-situ DEPORA experiment", Proceedings of the Eurocorr 99 conference, J. Mietz, R. Polder, and B. Elsener Editors.

Smailos, E., M.A. Cuñado, I. Azkarate, B. Kursten, G. Marx. 2003. *Long-Term Performance of Candidate Materials for HLW/Spent Fuel Disposal Containers,* Report FZKA 6809, Contract No. FIKW-CT-2000-00004, FZK.INE, Karlsruhe, Germany.

Smailos, E., M.A. Cuñado, B. Kursten, I. Azkarate, G. Marx. 2004. *Long-Term Performance of Candidate Materials for HLW/Spent Fuel Disposal Containers, Final Report*, European Commission, 5th Euratom Framework Programme, Contract No. FIKW-CT-2000-00004, May, 2004.

Snider, A.C. 2003. "Verification of the Definition of Generic Weep Brine and the Development of a Recipe for This Brine." Analysis report, April 8, 2003. Carlsbad, NM: Sandia National Laboratories. ERMS 527505.

Sorensen, N.R. and M.A. Molecke. 1992. "Summary of the WIPP Materials Interface Interactions Test – Metal Corrosion", SAND92-1921C. Albuquerque, NM: Sandia National Laboratories.

Sugimoto, K., R. Dinnebier, and J. Hanson. 2007. Structures of three dehydration products of bischofite from in situ synchrotron powder diffraction data ($MgCl_2.nH_2O$; n = 1, 2, 4). *Acta Crystallographica Section B, B63*, 235-242.

Telander, M., and R. Westerman. 1993. *Hydrogen Generation by Metal Corrosion in Simulated Waste Isolation Pilot Plant Environments: Progress Report for the Period November 1989 through December 1992.* SAND92-7347, Albuquerque, NM: Sandla National Laboratories.

Telander, M., and R. Westerman. 1997. *Hydrogen Generation by Metal Corrosion in Simulated Waste Isolation Pilot Plant Environments.* SAND96–2538, Albuquerque, NM: Sandia National Laboratories.

van Middlesworth, J.M., and S.A. Wood. 1999. The stability of palladium(II) hydroxide and hydroxy-chloride complexes: An experimental solubility study at 25-85 ^{o}C and 1 bar. Geochimica et Cosmochimica Acta 63, 1751-1765.

Wall, N., and D. Enos. 2006. *Iron and Lead Corrosion in WIPP-Relevant Conditions.* ERMS 543238, TP 06 02, Rev.1, Carlsbad, NM: Sandia National Laboratories.

Weck, P. F., E. Kim, C.F. Jove-Colon, D.C. Sassani. 2012. Structures of uranyl peroxide hydrates: a first-principles study of studtite and metastudtite. *Dalton Trans.* **41**, 9748-9752.

Westerman, R. E., J.H. Haberman, S.G. Pitman, B.A. Pulsipher, and L.A. Sigalla. 1986. *Annual report—FY 1984: Corrosion and environmental-mechanical characterization of iron-base nuclear waste package structural barrier materials*. PNL-5426, Richland, WA: Pacific Northwest National Laboratory.

Westerman, R. E., J.H. Haberman, S.G. Pitman, K.H. Pool, K.C. Rhoads, and M.R. Telander. 1988. *Salt repository project. Annual report–FY 1986. Corrosion behavior of A216 grade WCA mild steel and titanium grade 12 alloy in hydrothermal brines*. PNL/SRP-6221, Richland, WA: Pacific Northwest National Laboratory.

Wilson, T. P. and D.T. Long. 1993. Geochemistry and Isotope Chemistry of Michigan Basin Brines; Devonian Formations, *Applied Geochemistry*, *8*, 81-100.

Wolery, T.W., Y.-L. Xiong, and J. Long. 2010. Verification and Validation Plan/Validation Document for EQ3/6 Version 8.0a for Actinide Chemistry, Document Version 8.10. Carlsbad, NM: Sandia National laboratories. ERMS 550239.

Xiong, Y. 2008. "Preparing Synthetic Brines for Geochemical Experiments". Activity/Project Specific Procedure SP 20-4 Revision 2. Albuquerque, NM: Sandia National Laboratories. https://nwmp.sandia.gov/onlinedocuments/nwmp/sp/sp2004.pdf.

Xiong, Y, C. Jové Colón, and Y. Wang. 2012. *Test Plan for Determining Thermodynamic Properties of Brines, Minerals and Corrosion Products for High Level Radioactive Waste Disposal in Salt.* FCRD-UFD-2012-000339.